ATMS 533 Notes on Single-Scattering

Table of Contents

Review of Electromagnetism

References for EM theory

DJ Griffiths 1981 Introduction to Electrodynamics Chap 8

JT Houghton & SD Smith 1966 Infrared Physics pp 5-11

Reitz, Milford, Christy 1980 Foundations of Electromagnetic Theory.

References for Polarized Light

Shurcliff & Ballard 1964 Polarized Light

van de Hulst pp 40-44

Chandrasekhar pp 24-35

Liou ~~~~ sec. 6.6 (second edition)

A. Electric field

Coulomb's law: The force between two charges q and Q is proportional to q, Q, $\frac{1}{r^2}$

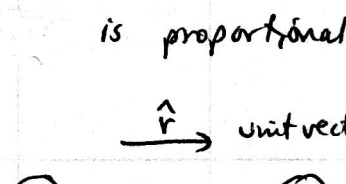

$$\hat{r} = \frac{\bar{r}}{|\bar{r}|}$$

F in Newtons, q in coulombs, r in meters.

$$\bar{F} = \frac{1}{4\pi\epsilon_0} \frac{qQ}{r^2} \hat{r} \qquad \text{where} \quad \epsilon_0 = 8.85 \times 10^{-12} \ \frac{\text{coul}^2}{\text{Nm}^2}$$

One electron has charge of 1.6×10^{-19} coulombs.

Electric field.

For an assemblage of charges, the individual forces can be added. The net force on Q is described by an "electric field" $\bar{E}$, defined as

$\bar{F} = Q\bar{E}$, where $\bar{F}$ is the force produced on charge Q.

$\bar{E}$ has units $\frac{\text{newtons}}{\text{coulomb}}$ or $\frac{\text{volts}}{\text{meter}}$.

Definition of volt: $\text{volt} \equiv \frac{\text{newton} \cdot \text{meter}}{\text{coulomb}}$.

For example

$$\bar{E} = \frac{1}{4\pi\epsilon_0} \frac{q}{r^2} \hat{r}$$ if one charge produces the electric field

or $$\bar{E} = \frac{1}{4\pi\epsilon_0} \sum_i \frac{q_i}{r_i^2} \hat{r}_i$$ for an assemblage of charges.

$\bar{E}$ diverges from (+) charge, and $|E|$ decreases with distance from the charge q

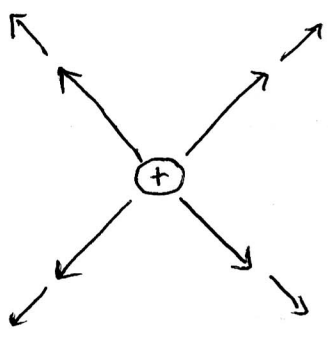

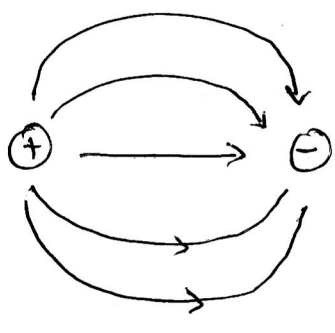

Gauss's Law.

is a restatement of the definition of electric field, using the "divergence theorem" of vector calculus

$$\nabla \cdot \bar{E} = \frac{\rho}{\epsilon_0} \qquad \text{where } \rho \text{ is charge-density in coulombs/m}^3 \qquad (1)$$

This is the differential form of Gauss's Law.

The integral form is

$$\int \bar{E} \cdot d\bar{a} = \frac{1}{\epsilon_0} Q_{enc} \qquad \text{where } da \text{ is area-element}$$

where the integration is over a closed surface and Q_{enc} is the enclosed charge.

Behavior of matter in electric field.

Contrast two types of material:

conductors: electrons free to move

dielectrics: electrons bound to molecules.

In response to an electric field,

in conductors: electrons will flow.

in dielectrics: permanent dipoles (polar molecules) will tend to align with the field;
dipoles will be induced in nonpolar molecules, also aligned with the field.

Dipole moment

Two equal and opposite charges separated by distance s have dipole moment

$\bar{p} = q s \hat{r}$.

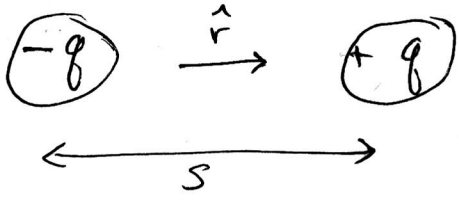

$\bar{p}$ points from $\ominus$ to $\oplus$; has units coulomb · meter.

Induced dipole in atoms.

Dipole moment is proportional to $\bar{E}$

$\bar{p} = \alpha \bar{E}$; α is the "atomic polarizability"

Bulk material

has permanent dipoles (partly aligned) and induced dipoles. Describe it by its average dipole moment:

Define Polarization $\bar{P}$ = dipole moment per unit volume.

$\bar{P}$ has units $\frac{\text{coul. meter}}{m^3}$

A divergence of polarization (i.e. if P changes with location in the material) corresponds to a net accumulation of bound charge:

$$\rho_b = -\bar{\nabla}\cdot\bar{P}$$ where ρ_b is density of bound charge $\left(\frac{coul}{m^3}\right)$

Gauss' law applied to dielectric material, separating free and bound charges: $\bar{\nabla}\cdot\bar{E} = \rho/\epsilon_0$

$$\epsilon_0\bar{\nabla}\cdot\bar{E} = \rho = \rho_{free} + \rho_{bound} = -\bar{\nabla}\cdot\bar{P} + \rho_{free}$$

or $$\bar{\nabla}\cdot\underbrace{(\epsilon_0\bar{E} + \bar{P})}_{\downarrow} = \rho_f$$ Gauss' law in matter (2)

call this the Electric Displacement D (same units as $\bar{P}$)

units $\frac{coul\cdot m}{m^3}$ $\qquad \bar{D} = \epsilon_0\bar{E} + \bar{P}$

so $$\boxed{\bar{\nabla}\cdot\bar{D} = \rho_f}$$ (3)

It is useful to define $\bar{D}$ this way, because in the common situation of no free charges;

$$\bar{\nabla}\cdot\bar{D} = 0$$ (4)

(valid in low and middle atmosphere; not valid in magnetosphere)

Response of bulk material to imposed electric field

By analogy to the atomic polarizability, we define the electric susceptibility χ_e which describes the response of bulk material to $\bar{E}$:

$$\bar{P} = \chi_e \epsilon_0 \bar{E} \qquad (5)$$

χ_e is unitless, because $\epsilon_0 E$ & P have the same units.
If the medium is isotropic, $\bar{P} \parallel \bar{E}$ so χ_e is a scalar.

If χ_e is a scalar then $\bar{D}$ is also proportional to $\bar{E}$, as follows:

$$\bar{D} = \epsilon_0 \bar{E} + \bar{P} = \epsilon_0 \bar{E} + \epsilon_0 \chi_e \bar{E} = \underbrace{\epsilon_0 (1 + \chi_e)}_{\text{"permittivity" } \epsilon} \bar{E}$$

so $\boxed{\bar{D} = \epsilon \bar{E}}$; ϵ is a roundabout way of describing the response of the medium to $\bar{E}$. (6)

$$\epsilon = \epsilon_0 \underbrace{(1 + \chi_e)}_{\text{dielectric constant} = \epsilon/\epsilon_0 = \text{relative permittivity} = \epsilon_{rel}} \qquad (7)$$

↙ permittivity

(unitless)

so ϵ_0 is called the "permittivity of free space"

examples of ϵ/ϵ_0 for static electric field:

material	ϵ/ϵ_0	χ_e
vacuum	1	0
air	1.05	0.05
glass	4-7	3-6
water	~80	79

B. Magnetic field

For magnetic field, relationships are analogous to electric field.

1. Biot-Savart Law

Currents flowing in two nearby wires cause a force between them.

This can be described by a field: The moving charges in wire 1 create a magnetic field which causes a force on wire 2 if charges are moving in wire 2.

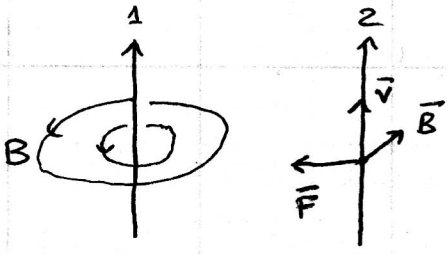

The magnetic field $\bar{B}$ is given by the Biot-Savart Law.

If charges Q in wire 2 are moving at velocity V then

$$\bar{F} = Q(\bar{v} \times \bar{B}).$$ Analog of coulomb's law. (8)

Define: current I = charge per unit time $\frac{\text{coul}}{\text{sec}}$ = ampere

current per unit area $\bar{J}$ or "current density",

charge crossing unit area in unit time. $\frac{\text{ampere}}{m^2} = \frac{\text{coul/sec}}{m^2}$

2. Ampere's law

Using the definition of J, together with Biot-Savart Law, we obtain Ampere's law for magnetic field

(analog of Gauss' law for electric field)

Ampères law:

$$\boxed{\bar{\nabla} \times \bar{B} = \mu_0 \bar{J}} \quad \text{or} \quad \frac{\bar{\nabla} \times \bar{B}}{\mu_0} = \bar{J} \qquad (9)$$

units of B : $\frac{\text{newtons}}{\text{amp} \cdot \text{meter}}$

I.e. a current $\bar{J}$ causes a magnetic field $\bar{B}$.

$\mu_0 = 4\pi \times 10^{-7} \frac{N}{\text{amp}^2}$

[Units of B/μ_0 :

$\frac{N}{\text{amp} \cdot m} \times \frac{\text{amp}^2}{N} = \frac{\text{amp}}{m} = \frac{\text{amp} \cdot m^2}{m^3}$]

Magnetic field in matter

A magnetic dipole is caused by a current-orbit

(units amp m^2 ; current x area enclosed)

E.g. an electromagnet

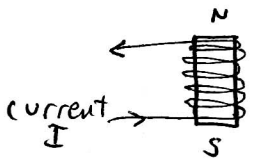

An imposed magnetic field creates a torque on a magnetic dipole and causes it to align with the magnetic field.

Define magnetization $\bar{M}$ (in analogy to $\bar{P}$), the magnetic dipole moment per unit volume, units $\frac{\text{amp} \cdot m^2}{m^3}$, i.e. same units as B/μ_0. It corresponds to "bound currents" J_b :

$$\bar{J}_b = \bar{\nabla} \times \bar{M}.$$

so $$\frac{\bar{\nabla} \times \bar{B}}{\mu_0} = \bar{J} = \bar{J}_f + \bar{J}_b = \bar{J}_f + \bar{\nabla} \times \bar{M}$$

so $$\bar{\nabla} \times \left(\frac{\bar{B}}{\mu_0} - \bar{M} \right) = \bar{J}_f \qquad \text{Ampères law in matter.} \qquad (10)$$

Although Eq (10) accurately describes most laboratory experiments, it is incomplete, as shown by Maxwell. To the r.h.s. should be added the "displacement current" $\frac{\partial \bar{D}}{\partial t}$:

$$\bar{\nabla} \times \underbrace{\left(\frac{\bar{B}}{\mu_0} - \bar{M}\right)}_{\text{call this } \bar{H}} = \bar{J}_f + \frac{\partial \bar{D}}{\partial t} \qquad \text{"Maxwell-Ampere law"} \qquad (11)$$

$\frac{\partial \bar{D}}{\partial t}$ has units of current density: $\frac{\text{coul. m}}{\text{m3 sec}} = \frac{\text{amp}}{\text{m}^2}$

Response of matter to an imposed magnetic field

By analogy to electric susceptibility, define <u>magnetic susceptibility</u> χ_m:

$$\bar{M} = \chi_m \bar{H} \qquad \text{This relation describes a "linear" material.} \qquad (12)$$

Then $\bar{B}$ is related to $\bar{H}$ as

$$\bar{B} \equiv \mu_0 (\bar{H} + \bar{M}) = \underbrace{\mu_0 (1 + \chi_m)}_{\text{"magnetic permeability" } \mu} \bar{H}$$

so $B = \mu H$

$$\mu = \mu_0 (1 + \chi_m)$$

χ_m: magnetic susceptibility

μ: permeability

$(1 + \chi_m)$: relative permeability $\frac{\mu}{\mu_0} \approx 1.0$ for nonmagnetic materials

μ_0 is called "permeability of free space"

C. Conductivity

Real materials are intermediate between dielectrics & conductors.

The induced free current density $\bar{J}_f$ caused by an electric field $\bar{E}$ is proportional to $\bar{E}$. The proportionality constant is σ, the "conductivity"

$$\bar{J}_f = \sigma \bar{E} \qquad (13)$$

Units of J_f: amp/m^2

units of E: $\frac{\text{volt}}{m}$ or $\frac{\text{newtons}}{\text{coulomb}}$

units of σ: $\frac{\text{ampere}}{\text{volt} \cdot \text{meter}}$ or $\frac{\text{amp} \cdot \text{coul}}{\text{newton} \cdot m^2}$

D. Maxwell's equations

(14) $\bar{\nabla} \cdot \bar{D} = \rho_f$ Gauss's Law. $\rho_f \approx 0$ in lower atmosphere; $\rho_f \neq 0$ in plasma. (magnetosphere)

(15) $\bar{\nabla} \cdot \bar{B} = 0$ No magnetic monopoles.

(16) $\bar{\nabla} \times \bar{E} = -\frac{\partial \bar{B}}{\partial t} = -\mu \frac{\partial \bar{H}}{\partial t}$ Faraday's law. A changing magnetic field induces an electric field.

(17) $\bar{\nabla} \times \bar{H} = J_f + \frac{\partial \bar{D}}{\partial t} = \sigma \bar{E} + \epsilon \frac{\partial \bar{E}}{\partial t}$ Ampère - Maxwell equation. A changing electric field induces a magnetic field.

$J_f = \sigma E$
$D = \epsilon E$

E. Electromagnetic waves

Maxwell's equations allow for the possibility of propagating electromagnetic waves, because of (16) & (17).

We examine solutions in the form of plane waves; ie that depend on time and only a single space coordinate z but not x, y. This is the situation at great distance from the source, which could be an oscillating dipole.

Apply $\bar{\nabla} \times$ to eq (16) to obtain a differential equation for $\bar{E}$

$$\text{LHS} = \nabla \times (\nabla \times \bar{E}) = -\nabla^2 E + \underbrace{\nabla(\nabla \cdot E)}_{\downarrow} = -\nabla^2 E$$

$\nabla \cdot E = \frac{1}{\epsilon} \nabla \cdot D = 0$ by (14)

↑ if not in the magnetosphere

$$\text{RHS} = -\nabla \times \frac{\partial B}{\partial t} = -\frac{\partial}{\partial t} \nabla \times B = -\mu \frac{\partial}{\partial t} \nabla \times H$$

Substitute (17) for $\nabla \times H$

$$= -\mu\sigma \frac{\partial \bar{E}}{\partial t} - \mu\epsilon \frac{\partial^2 \bar{E}}{\partial t^2}$$

so $$\boxed{\nabla^2 \bar{E} - \mu\epsilon \frac{\partial^2 \bar{E}}{\partial t^2} - \mu\sigma \frac{\partial \bar{E}}{\partial t} = 0} \qquad (18)$$

Eq (18) describes a damped wave. If $\sigma = 0$ it is undamped (in free space or a dielectric)

For a plane wave, E varies only in z not (x, y)

so $\nabla^2 E = \frac{\partial^2}{\partial z^2} \bar{E}$ and

$$\boxed{\frac{\partial^2 \bar{E}}{\partial z^2} - \mu\epsilon \frac{\partial^2 \bar{E}}{\partial t^2} - \mu\sigma \frac{\partial \bar{E}}{\partial t} = 0} \qquad (19)$$

Try a solution to (19): $\bar{E} = \bar{E}_0 \, e^{i\omega t - ikz - i\gamma}$ (20)

where k is to be determined.

⊕ z is the direction of propagation.

ω is the oscillation rate of the dipole; gives the variation of E with time at one point. ω is in radians/sec

so the oscillation rate ν in cycles per second is $\nu = \frac{\omega}{2\pi}$

k is the propagation constant; describes how E varies in space at any one time

γ is a phase.

From (20):

$$\frac{\partial \bar{E}}{\partial z} = -ik\bar{E}$$

$$\frac{\partial^2 \bar{E}}{\partial z^2} = i^2 k^2 \bar{E} = -k^2 E$$

$$\frac{\partial \bar{E}}{\partial t} = i\omega \bar{E}$$

$$\frac{\partial^2 \bar{E}}{\partial t^2} = -\omega^2 E$$

} first & second derivatives in space and time.

putting these into (19):

$$-k^2\bar{E} + \mu\epsilon\omega^2\bar{E} - \mu\sigma i\omega\bar{E} = 0 \qquad (21)$$

Eq (21) can be solved for k, giving the possible values of k which will satisfy (19). From (21):

$$-k^2 + \mu\epsilon\omega^2 - \mu\sigma i\omega = 0$$

$$\text{or} \quad \frac{k^2}{\omega^2} = \mu\epsilon\left(1 - \frac{\sigma i}{\epsilon\omega}\right) \qquad (22)$$

Now introduce the <u>phase speed</u> c of the wave:

Following a wave crest (constant $\bar{E}$), in (20),

the exponent $i\omega t - ikz - i\gamma = \text{constant}$

Then $$c \equiv \frac{dz}{dt} = \frac{\omega}{k} \quad \text{or} \quad k = \frac{\omega}{c} = \frac{2\pi}{\lambda},$$

where λ is wavelength,

because $$\lambda = \frac{c}{\nu} = \frac{2\pi c}{\omega} \quad \text{so} \quad \frac{\omega}{c} = \frac{2\pi}{\lambda}.$$

From (22), $$c = \frac{\omega}{k} = \left[\mu\epsilon\left(1 - \frac{\sigma i}{\epsilon\omega}\right)\right]^{-1/2} \qquad (23)$$

In free space $\left\{ \begin{array}{l} \sigma = 0 \\ \mu = \mu_0 \\ \epsilon = \epsilon_0 \end{array} \right\}$ so $c_0 = (\mu_0 \epsilon_0)^{-1/2} = 3 \times 10^8 \frac{m}{sec}$

Refractive index

Relate (23) to the refractive index m.

m is the ratio of speed of wave in a vacuum to speed in material.

$$m^2 \equiv \frac{c_0^2}{c^2} = \frac{k^2}{\omega^2 \epsilon_0 \mu_0} = \frac{\mu \epsilon}{\mu_0 \epsilon_0} \left(1 - \frac{i\sigma}{\omega \epsilon}\right) = \mu_{rel} \epsilon_{rel} \left(1 - \frac{i\sigma}{\omega \epsilon_{rel} \epsilon_0}\right)$$

For nonmagnetic material $\mu_{rel} = 1$ so

$$m^2 = \epsilon_{rel} \left(1 - \frac{i\sigma}{\omega \epsilon_{rel} \epsilon_0}\right) = \underbrace{\left[\epsilon_{rel} - \frac{i\sigma}{\omega \epsilon_0}\right]}$$

This is the "complex relative permittivity" or "complex dielectric constant" ϵ_{cx}

So the refractive index m is also a complex number

$$m_{cx} = \sqrt{\epsilon_{cx}}$$

$$m = m_{cx} = m_{re} - i m_{im}$$

If the imaginary part is zero there is no attenuation. The imaginary part of ϵ_{cx} is proportional to σ, the conductivity. So conductivity causes attenuation (absorption) of the wave.

m_{im} will turn out to be proportional to the absorption coefficient, as we now show.

Substitute into the trial solution (20) the propagation vector $k = \frac{\omega}{c} = \frac{\omega m}{c_0}$.

$$\bar{E} = E_0 e^{i\omega t - i\gamma} e^{-ikz}$$

$$e^{-ikz} = e^{-i\frac{\omega m}{c_0} z} = e^{-\frac{i\omega}{c_0}(m_{re} - i m_{im})z}$$

$$= e^{-\frac{i\omega}{c_0} m_{re} z} e^{-\omega \frac{m_{im}}{c_0} z}$$

So

$$\bar{E} = \bar{E}_0 \underbrace{e^{i\omega t - i\gamma} e^{-\frac{i\omega}{c_0} m_{re} z}}_{\text{oscillating}} \underbrace{e^{-\omega \frac{m_{im}}{c_0} z}}_{\text{attenuation}} \qquad (24)$$

Now relate m_{im} to absorption coefficient $\sigma_{abs}\ (m^{-1})$:

First replace ω by λ:

$$\lambda = \frac{c}{\nu} = \frac{2\pi c}{\omega}\ ; \quad \frac{\omega}{c} = \frac{2\pi}{\lambda} \qquad \frac{\omega}{c_0} = \frac{2\pi}{\lambda_0}$$

$$e^{-\omega \frac{m_{im}}{c_0} z} = e^{-\left(\frac{2\pi m_{im}}{\lambda_0}\right) z}$$

Amplitude of electric vector $|E|$:

$$\frac{|E|}{|E_0|} = e^{-\left(\frac{2\pi m_{im}}{\lambda_0}\right) z}$$

We'll show that Flux $\propto |E|^2$, so

$$\frac{F(z)}{F(0)} = \frac{|E|^2}{|E_0|^2} = e^{-(4\pi m_{im}/\lambda_0) z} = e^{-\sigma_{abs} z}.$$

so $\boxed{\sigma_{abs} = \frac{4\pi m_{im}}{\lambda_0}}$ (units m^{-1}) (25)

σ_{abs} is absorption per meter

m_{im} is unitless, "absorption per wave"

JOURNAL OF GEOPHYSICAL RESEARCH, VOL. 113, D14220, doi:10.1029/2007JD009744, 2008

Optical constants of ice from the ultraviolet to the microwave: A revised compilation

Stephen G. Warren[1] and Richard E. Brandt[1]

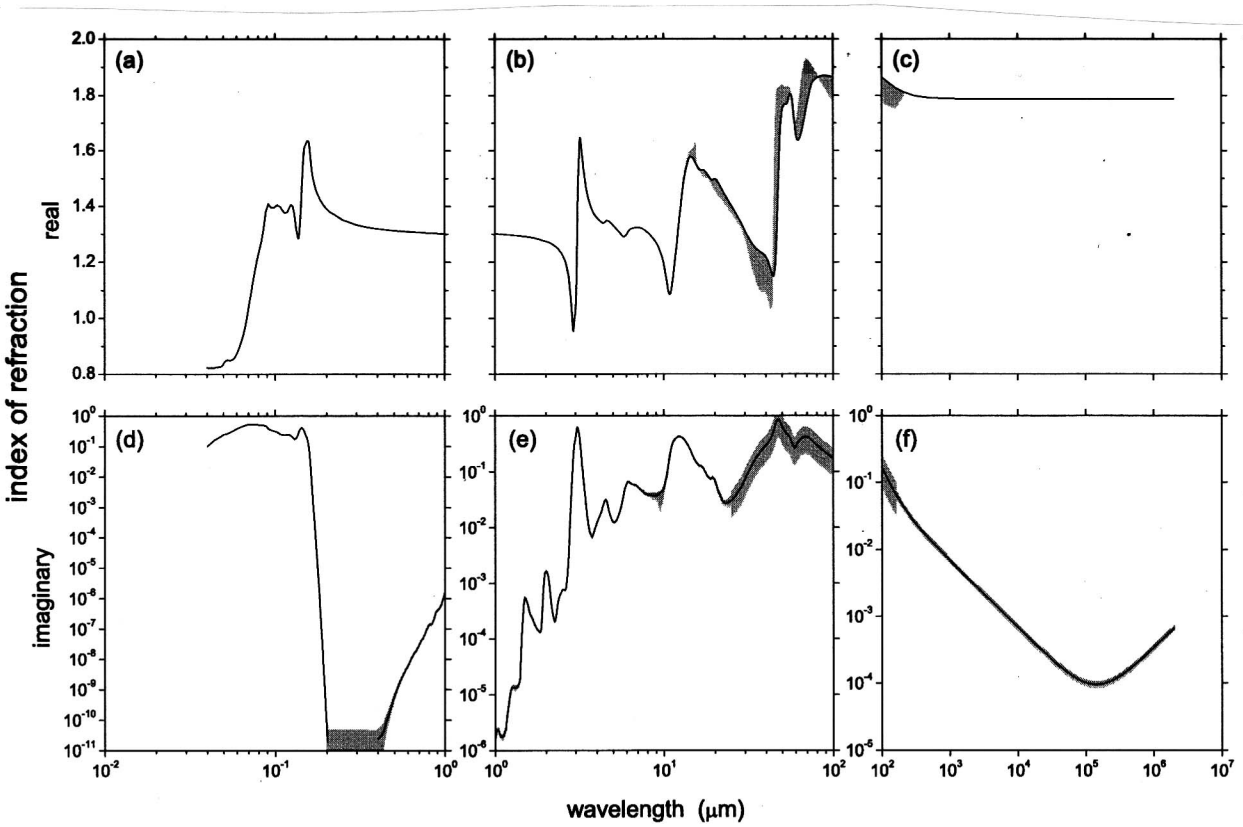

Figure 9. Compilation of the (a)–(c) real and (d)–(f) imaginary parts of the complex index of refraction of ice Ih at temperature 266 K. Uncertainty is indicated by the shading.

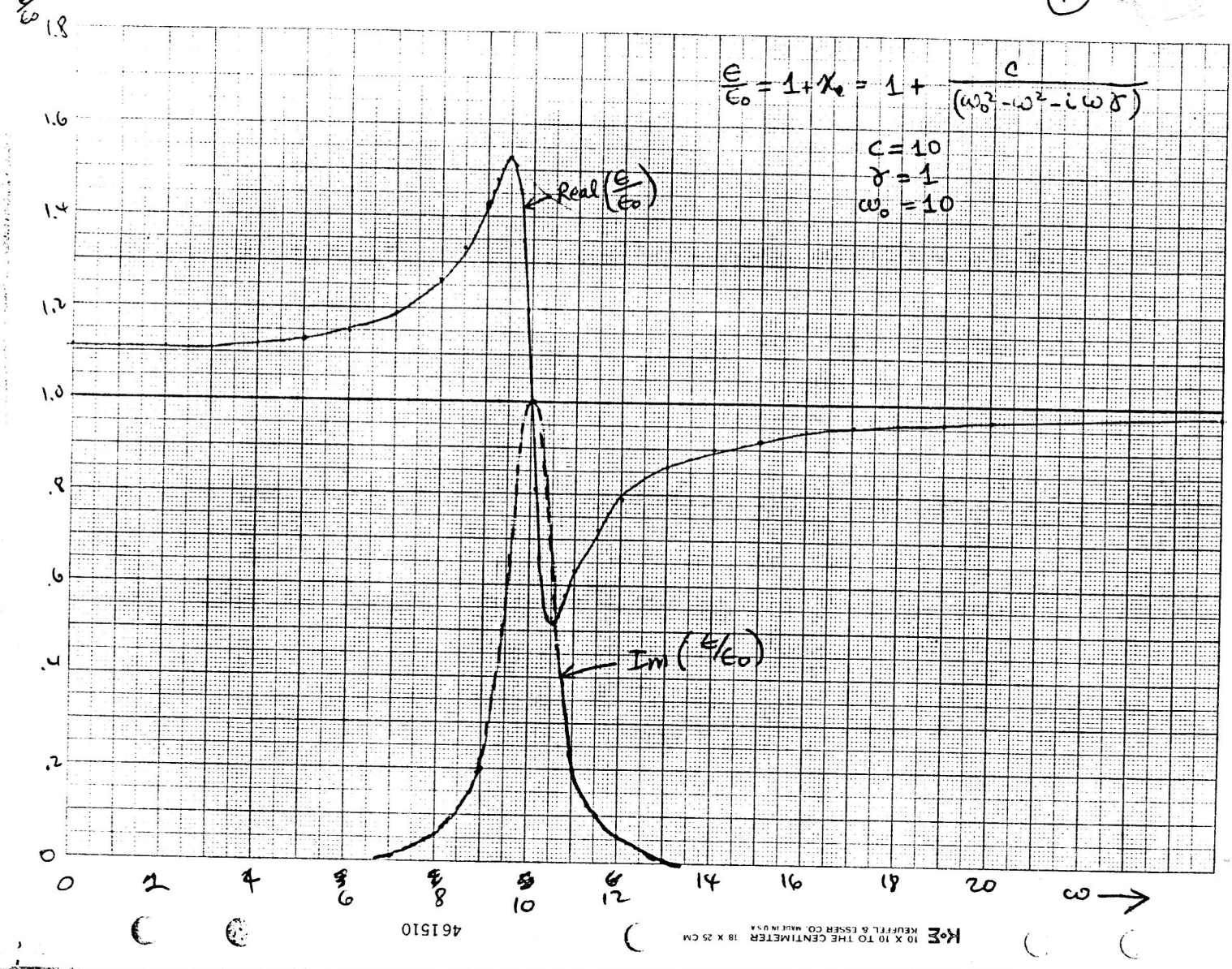

J. Geophys. Res. 76, 4924 (1971)

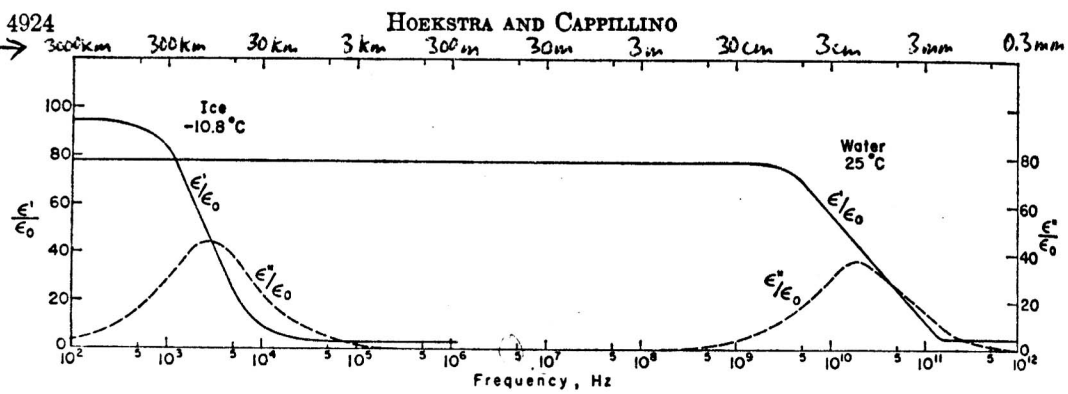

$\epsilon' = \epsilon_{re}$

$\epsilon'' = \epsilon_{im}$

Fig. 3. The dielectric behavior of ice [after *Auty and Cole*, 1952] and water [after *Collie et al.*, 1948] as a function of frequency.

By "theory of optical constants", we mean an explanation for the frequency-dependence of permittivity ε and conductivity σ. It is a classical theory. References are Jackson, *Classical Electrodynamics*, sec. 7.5, and Griffiths, *Introduction to Electrodynamics,* sec. 8.4.

ε, (μ), σ describe the response of the material to electric (and magnetic) fields. The response can depend on the driving frequency ω. A model for the behavior of electrons in matter gives σ(ω) and ε(ω). For most materials $\mu \approx \mu_o \neq f(\omega)$.

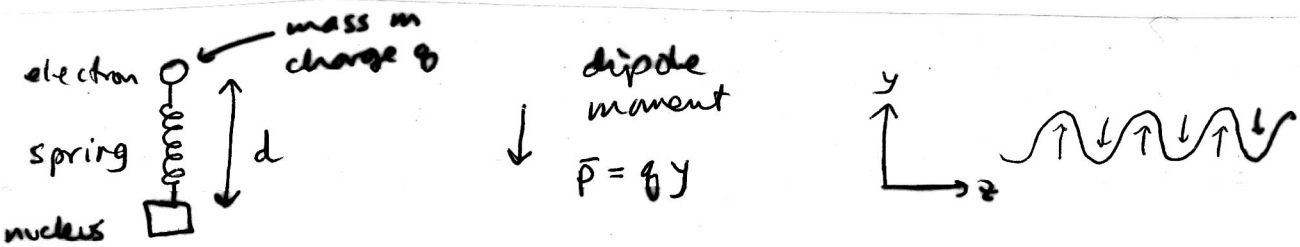

The EM wave causes an oscillating force in the y-direction. The dipole will tend to line up with the electric field.

Assume:

(1) d « λ, so that the whole atom sees the same phase of $\overline{E}$ (not true for X-rays).

(2) Magnetic force « electric force:

$$F = F_{elec} + F_{mag} = q\overline{E} + q\bar{v} \times \overline{B}.$$

We will show below on Page 24 that the magnitudes of B and E are related by $B = E/c$, so $F_{mag} \ll F_{elec}$ if v«c. The charge moves a distance d during one period (time λ/c), so the speed $v = d \cdot c/\lambda \ll c$ if $d \ll \lambda$.

There are three forces to consider:

(1) Restoring ("binding") force of spring, with spring constant k: $\boldsymbol{F_{bind} = -ky}$. Then the natural frequency of oscillation is $\omega_0 = \sqrt{k/m}$, so $k = m\omega_0^2$.

(2) "Frictional" damping when the electron moves, a force proportional to the velocity:

$$F_{damp} = -m\gamma \frac{dy}{dt}.$$

(3) External driving force of the incident wave $\overline{E}$ with frequency ω:

$F_{driv}=qE$

Now add the forces, and get an equation of motion for the electron, as *F=ma,* or *ma=F:*

$$m\frac{d^2y}{dt^2} = \underbrace{F_{bind}}_{-ky} + \underbrace{F_{damp}}_{-m\gamma\frac{dy}{dt}} + \underbrace{F_{driv}}_{+qE_0\cos\omega t}$$

$$-m\omega_0^2 y \qquad\qquad qE_0 e^{-i\omega t}$$

Divide by m, abbreviate $\frac{dy}{dt} \equiv \dot{y}$, use complex notation:-

$$\ddot{y} + \gamma\dot{y} + \omega_0^2 y = \frac{q}{m}E_0 e^{-i\omega t} \qquad (1)$$

(ω_0: natural frequency; ω: driving frequency)

The frequency of oscillation will be the frequency of the wave, ω. The amplitude of oscillation depends on both ω, ω_0. Maximum amplitude at $\omega = \omega_0$.

<u>Solution</u> of the differential equation (1) for $y(t)$, or for the dipole moment $p = qy$:

$$p(t) = \frac{q^2/m}{(\omega_0^2 - \omega^2) - i\gamma\omega} E_0 e^{-i\omega t} \qquad (2)$$

The imaginary term in the denominator causes p to be out of phase with E.

Eq (2) is the solution for one electron with natural frequency ω_0. Different electrons in the molecule have different natural frequencies ω_j and different damping coefficients γ_j. The dipole moment will be the sum of the individual contributions:

$$\bar{P} = \underbrace{\frac{q^2}{m}\left[\sum_j \frac{1}{(\omega_j^2 - \omega^2) - i\gamma_j\omega}\right]}_{\text{this is } \epsilon_0 \chi_e} \bar{E} \qquad (3)$$

And $\epsilon_{rel} = 1 + \chi_e$

$$\text{so} \quad \epsilon_{rel} = 1 + \frac{q^2}{m\epsilon_0} \sum_j \frac{1}{(\omega_j^2 - \omega^2) - i\gamma_j\omega} \qquad (4)$$

If ω_0 is far from ω, the imaginary part is small:

$$\gamma_j \omega \ll (\omega_j^2 - \omega^2)$$

so $\bar{P}$ is nearly in phase with $\bar{E}$ (or 180° out of phase if $\omega_j < \omega$).

If $\gamma = 0$ (no friction) then $\bar{P}$ and $\bar{E}$ are in phase for all frequency, but amplitude $\to \infty$ at $\omega = \omega_0$

Asymptotic behaviors at various points in the spectrum not close to any natural frequency ω_j (i.e. neglect $i\gamma_j\omega$ in denominator):

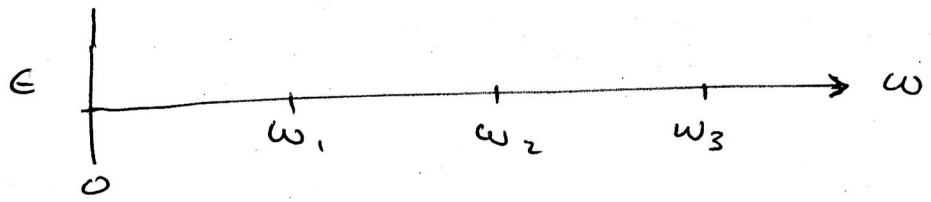

At $\omega < \omega_1$, all terms in the sum are positive;

$(\omega_j^2 - \omega^2) > 0$ for all j

At $\omega_1 < \omega < \omega_2$ there is one negative term.

As we pass each ω_j with increasing ω, we acquire an additional negative term.

Close to a natural frequency:

The real part of the denominator vanishes; the term in the sum is large and pure imaginary.

Amplitude of $\bar{P}$:

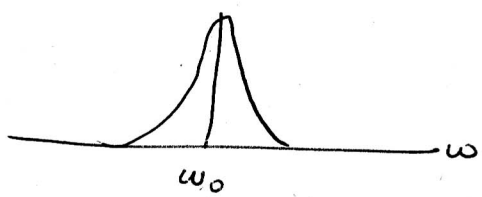

phase of $\bar{P}$ relative to $\bar{E}$:

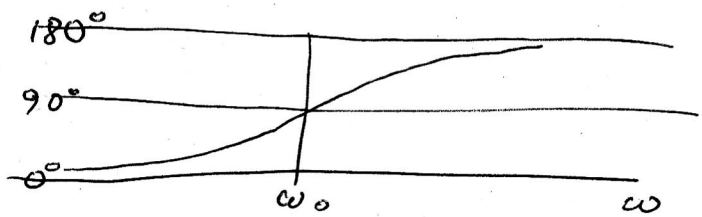

$$\text{phase} = \tan^{-1} \frac{\gamma\omega}{\omega_j^2 - \omega^2}$$

Behavior of ϵ_{re}, ϵ_{im} across ω_j :

See plot on page 17 for just one oscillator.

Example of <u>ice</u> : several natural frequencies ω_j

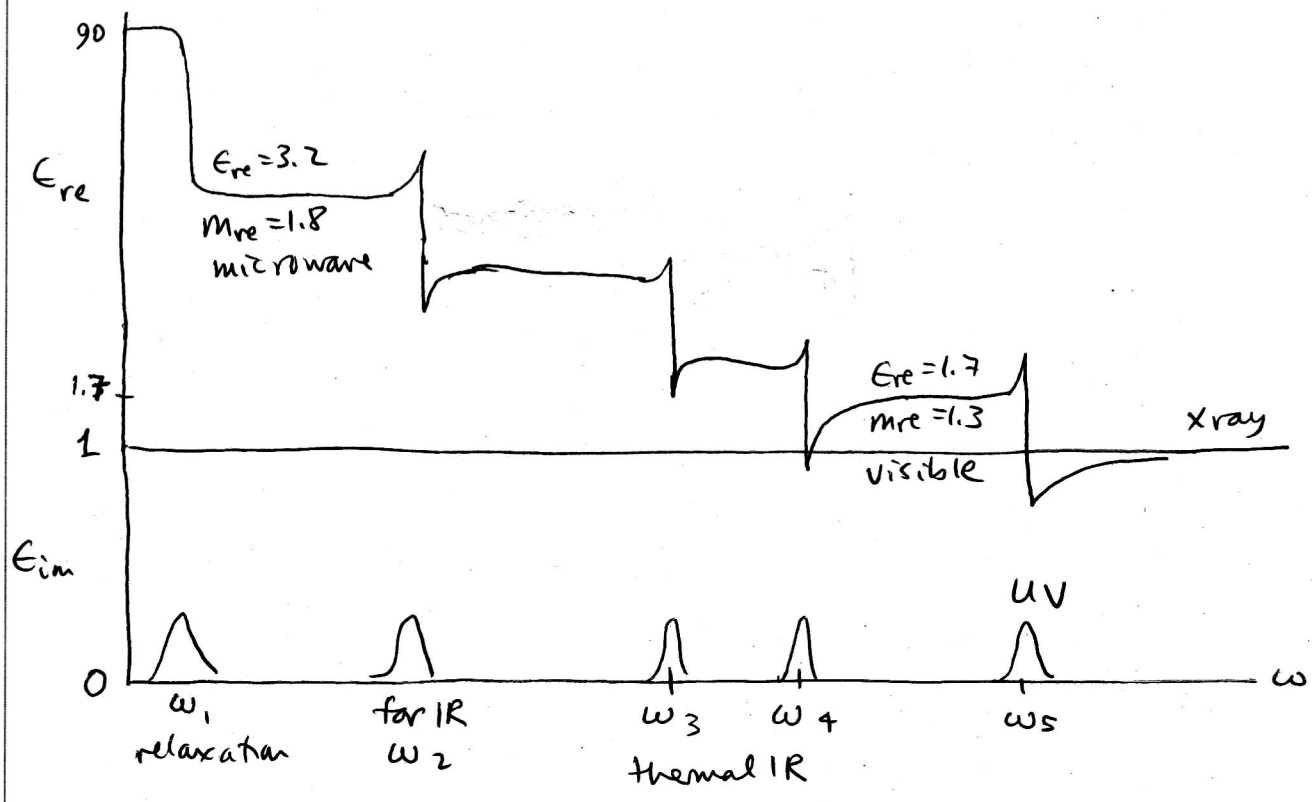

ϵ_{re} is related to $\int \epsilon_{im}\, d\omega$

by "dispersion relations", "Kramers-Kronig relations"

The response (ϵ) of the material to $\vec{E}$ at <u>any</u> frequency ω depends on <u>all</u> the natural frequencies ω_0.

This response is due to motion of bound electrons, so there is no absorption at $\omega = 0$.

In a "conductor" there are also free electrons, so they have $\omega_0 = 0$.

At all other frequencies there is no qualitative distinction between "conductors" and "dielectrics".

All materials have $\sigma \neq 0$, as a function $\sigma(\omega)$, but σ can be very low at some frequencies.

Electromagnetic waves

1. Show that $\bar{E}, \bar{H}, \bar{k}$ are mutually perpendicular.

Use $\bar{\nabla} \times \bar{E} = -\mu \frac{\partial \bar{H}}{\partial t}$ (16)

$\bar{\nabla} \to -i\bar{k}$; $\frac{\partial}{\partial t} \to i\omega$

So $-i\bar{k} \times \bar{E} = -i\omega\mu \bar{H}$

or $\bar{H} = \frac{\bar{k} \times \bar{E}}{\omega\mu}$ so $\bar{H}$ is $\perp$ the plane of $\bar{k}, \bar{E}$. (26)

Now to show $\bar{E} \perp \bar{k}$:

Use $\bar{\nabla} \times \bar{H} = \epsilon \frac{\partial \bar{E}}{\partial t} + \sigma \bar{E}$, put in $1 = -i^2$

$i\bar{k} \times \bar{H} = (\epsilon i\omega - i^2\sigma)\bar{E}$. cancel the i

so $\bar{E} = \frac{\bar{k} \times \bar{H}}{\epsilon\omega - i\sigma}$ so $\bar{E} \perp \bar{k}, \bar{H}$.

$\bar{k} \cdot \bar{E} = 0$
$\bar{k} \cdot \bar{H} = 0$
$\bar{H} \cdot \bar{E} = 0$

2. The magnitudes of $\bar{E}, \bar{B}$ are related.

From (26) $H = \frac{k}{\omega\mu} E$ so $B = \frac{k}{\omega} E = \frac{1}{c} E$

$\boxed{B = \frac{1}{c} E}$. The units of B, E differ by velocity.

electric force on charge Q $\bar{F} = Q\bar{E}$

magnetic force on moving charge $\bar{F} = Q(\bar{v} \times \bar{B})$

3. Energy per unit volume stored in EM field

$$U = \frac{1}{2}\left[\epsilon |E|^2 + \frac{1}{\mu}|B|^2\right] \qquad (27)$$

where U is in Joules/m^3. (Griffiths p. 289)

The first term is equivalent to the work required to assemble a charge distribution that will have electric field $\bar{E}$, against the force of coulomb repulsion. The second term is the work required to get currents going to establish a magnetic field B.

Since $B = \frac{1}{c}E$ and $c = \frac{1}{\sqrt{\mu\epsilon}}$ then $B^2 = \mu\epsilon E^2$

so (27) becomes $U = \frac{1}{2}(\epsilon E^2 + \epsilon E^2) = \epsilon E^2$ (28)

So the electric and magnetic fields each carry half the energy

4. Energy transported by EM field (at a point in space at an instant in time)

is given by Poynting vector

$$\bar{S} = \frac{1}{\mu} Re(\bar{E}_{cx}) \times Re(\bar{B}_{cx}), \text{ i.e. in direction } \bar{k}$$

But $B = \frac{1}{c}E$ and $c^2 = \frac{1}{\mu\epsilon}$ so $c\epsilon = \frac{1}{c\mu}$ so

$$\bar{S} = c\epsilon E^2 \hat{k}$$

$$\bar{S} = c U \hat{k} \qquad \bar{S} \text{ is a } \underline{\text{flux}} \ (W m^{-2}) \qquad (29)$$

↑ flux of energy; ↑ velocity; ↑ energy density

The average value of the magnitude of $\bar{S}$ is what is measured as energy flux. Average $\bar{S}$ over one wavelength:

$$U = \epsilon E^2 = \epsilon E_0^2 \cos^2(\omega t - kz - \gamma)$$

Avg value of $\cos^2$ is $\frac{1}{2}$. $\langle \cos^2 \rangle = 1/2$

So $\langle u \rangle = \frac{1}{2} \epsilon E_0^2$

and Flux $F = \langle S \rangle = c \langle U \rangle = \frac{1}{2} c \epsilon E_0^2$

$$\boxed{F = \tfrac{1}{2} c \epsilon E_0^2} \quad (W m^{-2}) \qquad (30)$$

Polarized Light

Define cartesian axes in the plane perpendicular to the direction of propagation

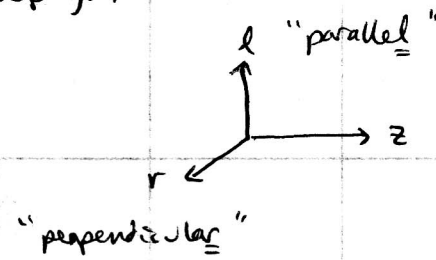

$\bar{E}$ is $\perp z$ but may have components in l, r directions:

$$\bar{E} = \hat{l} E_l + \hat{r} E_r \qquad (31)$$

where

$$\left.\begin{aligned} E_l &= a_l e^{i(\omega t - kz - \gamma_l)} \\ E_r &= a_r e^{i(\omega t - kz - \gamma_r)} \end{aligned}\right\} \quad (32)$$

The square of the magnitude of E is called I, the "intensity" but not to be confused with the radiative transfer term "intensity".

This I is proportional to Flux.

$$I = \langle E^* E \rangle \qquad \text{so} \qquad F = \tfrac{1}{2} c \epsilon I$$

so $\quad I_\ell = \langle E_\ell^* E_\ell \rangle$

$$I_r = \langle E_r^* E_r \rangle \qquad \text{and} \qquad I = I_\ell + I_r$$

The independent properties of a plane wave from (32) are $a_\ell, a_r, \gamma_\ell, \gamma_r$. But absolute phase is impossible to measure. Define $\delta \equiv \gamma_\ell - \gamma_r$. So the independent properties are $\underline{a_r, a_\ell, \delta}$. These determine the POLARIZATION of the EM wave

1. <u>Plane polarization</u>

a) $a_\ell = 0$;

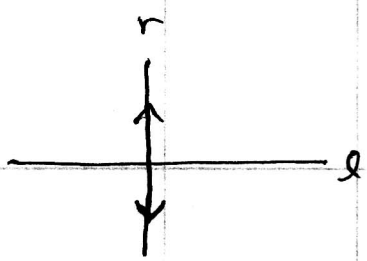

Electric vector oscillates along r

b) $a_r = 0$

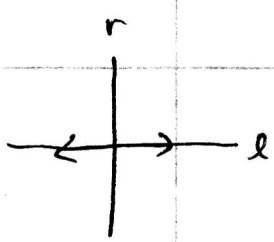

c) $a_\ell \neq a_r \neq 0$ $\quad \delta = 0$

$$\bar{E} = \left(\hat{\ell}\, a_\ell + \hat{r}\, a_r\right) e^{i(\omega t - kz)}$$

the "plane of polarization" is defined by the angle $\chi = \tan^{-1}\left(\frac{a_r}{a_\ell}\right)$

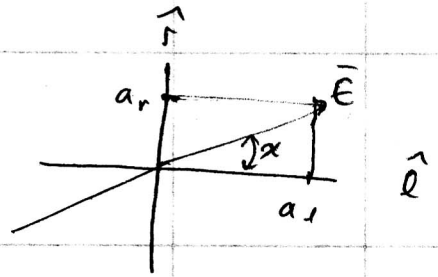

2. Circular polarization

$a_\ell = a_r = a$ $\quad \delta = \pm \pi/2$

$\bar{E}$ traces a circle. $\quad \bar{E} = a\left(\hat{\ell} + \hat{r}\, e^{\pm i \pi/2}\right) e^{i(\omega t - kz)}$

left circular polarization "lcp"

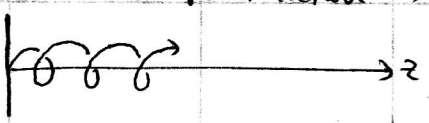

snapshot in time

$\delta = -\pi/2$

as seen by observer on z-axis looking toward source

right circular polarization "rcp":

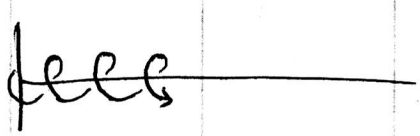

$\delta = +\pi/2$

Some authors use the opposite convention, labelling "lcp" for $\delta = +\pi/2$

3. Elliptical polarization

$\delta \neq n\pi/2$ $\quad a_l, a_r$ arbitrary.

for example if $a_l = a_r$, looking along z axis ~~back~~ toward source.

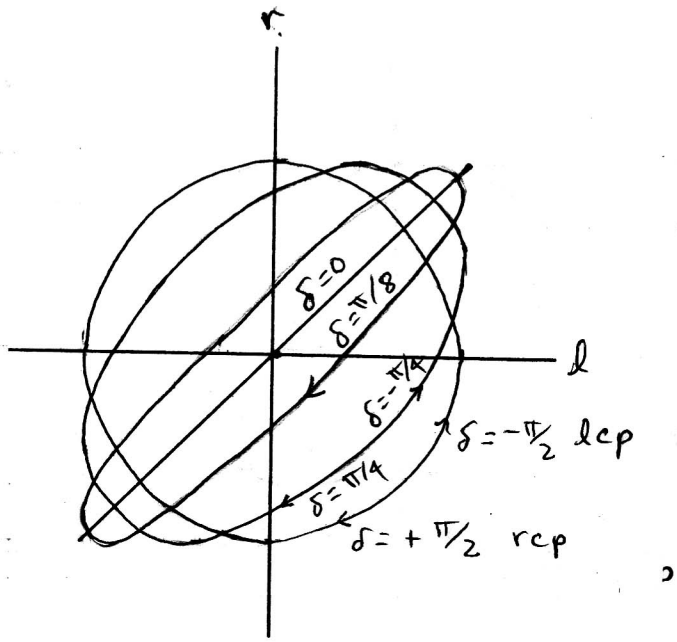

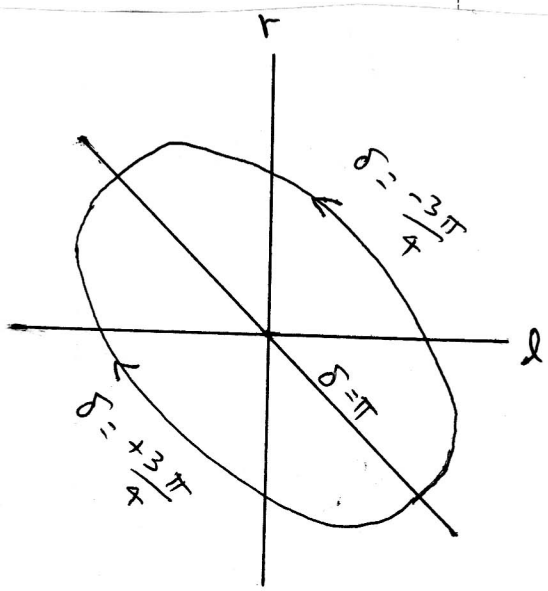

If $a_l \neq a_r$ then the major axis of the ellipse is not at 45°

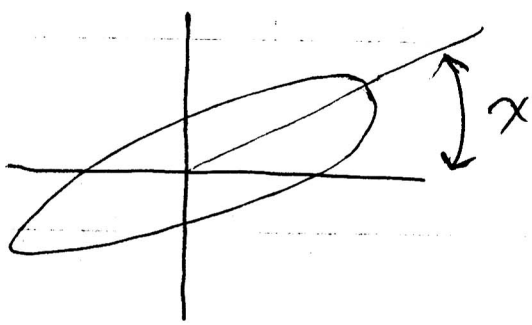

Since light can be partially polarized and partially unpolarized, we need 4 numbers (all of different units) to describe the state of polarization : a_l, a_r, δ, degree of polarization.

OR

"intensity"	proportional to flux	
plane of polarization	angle	
ellipticity	number	$\tan\beta = \frac{b}{a}$
degree of polarization	ratio	

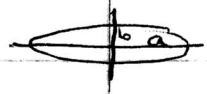

OR

These 4 quantities are combined into 4 parameters all with the same units : units of "intensity" ; i.e. $|E|^2$

STOKES PARAMETERS I, Q, U, V.

$$I = E_l E_l^* + E_r E_r^* = a_l^2 + a_r^2$$ (for completely polarized light)

$$Q = E_l E_l^* - E_r E_r^* = a_l^2 - a_r^2$$

$$U = Re(2E_l E_r^*) = 2a_l a_r \cos\delta$$

$$V = Im(2E_l E_r^*) = 2a_l a_r \sin\delta$$

If the light is completely polarized then $I^2 = Q^2 + U^2 + V^2$.

These 4 quantities are represented as the

Stokes vector $\bar{I} = \begin{pmatrix} I \\ Q \\ U \\ V \end{pmatrix}$

Unpolarized light

To say that light is unpolarized means that

$E_\ell(t)$ and $E_r(t)$ are uncorrelated.

There is then no systematic phase relation so $\langle\delta\rangle = 0$

and $\langle a_\ell^2\rangle = \langle a_r^2\rangle$, $\langle a_\ell\rangle = \langle a_r\rangle$

$$\langle\cos\delta\rangle = \langle\sin\delta\rangle = 0$$

E varies sporadically and randomly in time.

Then the time average of stokes vector (which is what is measured) is

$$I = \langle a_\ell^2 + a_r^2\rangle = I$$
$$Q = \langle a_\ell^2 - a_r^2\rangle = 0$$
$$U = \langle 2a_\ell a_r \cos\delta\rangle = 0$$
$$V = \langle 2a_\ell a_r \sin\delta\rangle = 0$$

Now normalize the Stokes vector to $I = 1$ and look at some examples. Q, U, and V will be in the range -1 to $+1$.

unpolarized $\begin{pmatrix}1\\0\\0\\0\end{pmatrix}$ ↔ $\begin{pmatrix}1\\1\\0\\0\end{pmatrix}$ ↙ $\begin{pmatrix}1\\0\\1\\0\end{pmatrix}$ ○ $\begin{pmatrix}1\\0\\0\\1\end{pmatrix}$

↕ $\begin{pmatrix}1\\-1\\0\\0\end{pmatrix}$ ↘ $\begin{pmatrix}1\\0\\-1\\0\end{pmatrix}$ ○ $\begin{pmatrix}1\\0\\0\\-1\end{pmatrix}$

note that $I = \sqrt{Q^2+U^2+V^2}$ for polarized light

$I > \sqrt{Q^2+U^2+V^2}$ for partially polarized light

$\sqrt{Q^2+U^2+V^2} = 0$ for unpolarized light.

Degree of polarization is $\dfrac{\sqrt{Q^2+U^2+V^2}}{I}$

Q gives the preference for vertical (-1) or horizontal $(+1)$ polarization

U gives the preference for $\pm 45°$ angle plane of polarization $(-1, +1)$

V gives the preference for circular as opposed to plane polarization
$(-1$ lcp $+1$ rcp$)$

Theorems for Stokes vector (proved by Chandrasekhar)

1. Stokes parameters can be added for two noninterfering beams

$$\begin{pmatrix}1\\1\\0\\0\end{pmatrix} + \begin{pmatrix}3\\0\\0\\3\end{pmatrix} = \begin{pmatrix}4\\1\\0\\3\end{pmatrix}$$

100% polarized + 100% polarized = 79% polarized

2. Unpolarized light can be resolved into two perpendicular polarized beams. (corollary of 1.)

$$\begin{pmatrix}I\\0\\0\\0\end{pmatrix} = \begin{pmatrix}I/2\\I/2\\0\\0\end{pmatrix} + \begin{pmatrix}I/2\\-I/2\\0\\0\end{pmatrix} \quad \text{or} \quad \begin{pmatrix}I/2\\0\\0\\I/2\end{pmatrix} + \begin{pmatrix}I/2\\0\\0\\-I/2\end{pmatrix}$$

3. Partially polarized light can be resolved into two beams, one unpolarized and the other completely polarized.

$$\begin{pmatrix} I \\ Q \\ U \\ V \end{pmatrix} = \begin{pmatrix} I - \sqrt{Q^2+U^2+V^2} \\ 0 \\ 0 \\ 0 \end{pmatrix} + \begin{pmatrix} \sqrt{Q^2+U^2+V^2} \\ Q \\ U \\ V \end{pmatrix}$$

4. Two beams with same IQUV cannot be distinguished experimentally, so the Stokes vector gives the complete specification.

To measure IQU need a polarizer and a detector

To measure V need also a retarder

eg a quarter-wave plate retards a_1 by 90°.

Any optical instrument can be represented as a 4×4 matrix "Müller matrix"

$$\begin{pmatrix} I' \\ Q' \\ U' \\ V' \end{pmatrix} = \begin{bmatrix} & & & \\ & & & \\ & & & \\ & & & \end{bmatrix} \begin{pmatrix} I \\ Q \\ U \\ V \end{pmatrix}$$

The scattering process will also be a 4×4 matrix.

Instead of the phase function $P(\cos\Theta)$ we have

a phase matrix $\underline{\underline{P}}(\cos\Theta)$

Each of the 16 elements of $\underline{\underline{P}}$ is a function of $\cos\Theta$.

REFLECTION AT AN INTERFACE
TRANSMISSION

[Griffiths chapter 8]

Maxwell's equations can be used to show what happens to an EM wave at a boundary between two materials of different σ, ϵ, μ

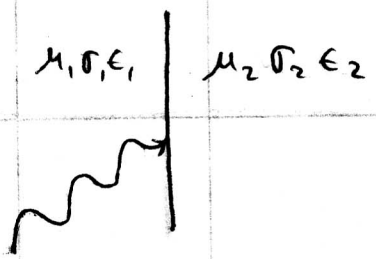

By applying Maxwell's equations to a small volume containing part of the boundary, one finds that the tangential components of $\bar{E}$ and $\bar{H}$ are continuous across the boundary. This also leads to energy conservation (shown by Bohren/Huffman)

The derivations are given in any textbook for EM.
Here we just give the results for successively more complicated situations:

1. normal incidence, $\sigma = 0$
2. oblique incidence, $\sigma = 0$
3. normal incidence, $\sigma \neq 0$
4. oblique incidence, $\sigma \neq 0$

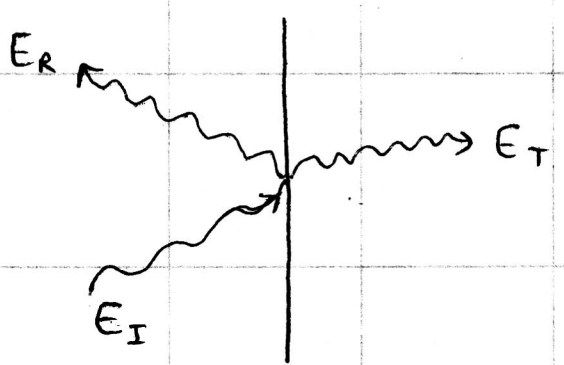

Define amplitudes of $\bar{E}$ fields as

E_I incident
E_R reflected
E_T transmitted

1. normal incidence, $\theta = 0$

$$\frac{E_R}{E_I} = \frac{1-m}{1+m} \qquad \frac{E_T}{E_I} = \frac{2}{1+m}$$

where m is ~~refractive~~ relative refractive index $\frac{n_2}{n_1} = m$

The energy flux transmitted & reflected is given by (30):

$$F = \tfrac{1}{2} \epsilon c E^2$$

Flux - Reflectance R and transmittance T are then

$$R = \left(\frac{E_R}{E_I}\right)^2 = \left(\frac{m-1}{m+1}\right)^2 \qquad (31)$$

$$T = \frac{\epsilon_2 c_2}{\epsilon_1 c_1} \frac{E_T^2}{E_I^2} = \frac{m^2}{m} \left(\frac{2}{1+m}\right)^2 = m\left(\frac{2}{1+m}\right)^2 \qquad (32)$$

so $R + T = 1$ as it must for energy conservation.

Examples ① air - glass interface $m = 1.5$ at visible wavelengths

$R = 0.04$

$T = 0.96$

2. Oblique incidence, $\sigma = 0$

Define ~~angle~~ zenith angles (angles from surface-normal)

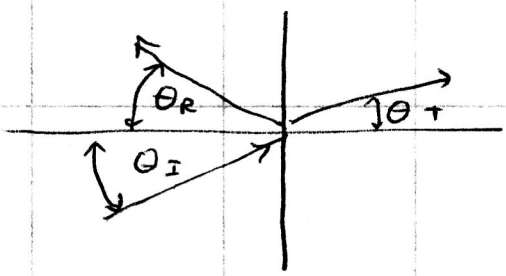

Results:

a) The three $\bar{k}$ vectors form a plane which includes the surface normal "plane of incidence"

b) $\theta_I = \theta_R$

c) $m_2 \sin\theta_T = m_1 \sin\theta_I$ (Snell's law)

d) E_R, E_T given by FRESNEL's equations

They differ for the two polarizations:

$E_\perp$ · perpendicular to plane of incidence

$E_\parallel$ parallel to plane of incidence.

example for $m = 1.5$, $E_\parallel$:

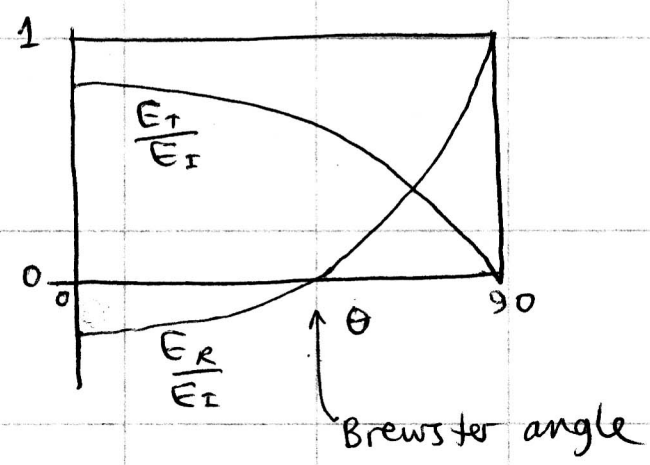

Fresnel's equations:

Define $m \equiv \frac{m_2}{m_1}$

$$R_{\parallel} = \left[\frac{\cos\theta_T - m\cos\theta_I}{\cos\theta_T + m\cos\theta_I} \right]^2$$

$$R_{\perp} = \left[\frac{\cos\theta_I - m\cos\theta_T}{\cos\theta_I + m\cos\theta_T} \right]^2$$

For unpolarized incidence,

$$R = (R_{\parallel} + R_{\perp})/2 .$$

Clouds in a Glass of Beer

Simple Experiments in Atmospheric Physics

CRAIG F. BOHREN

Pennsylvania State University

Foreword by
JEARL WALKER

1987

WILEY SCIENCE EDITIONS

JOHN WILEY & SONS, INC.

New York · Chichester · Brisbane · Toronto · Singapore

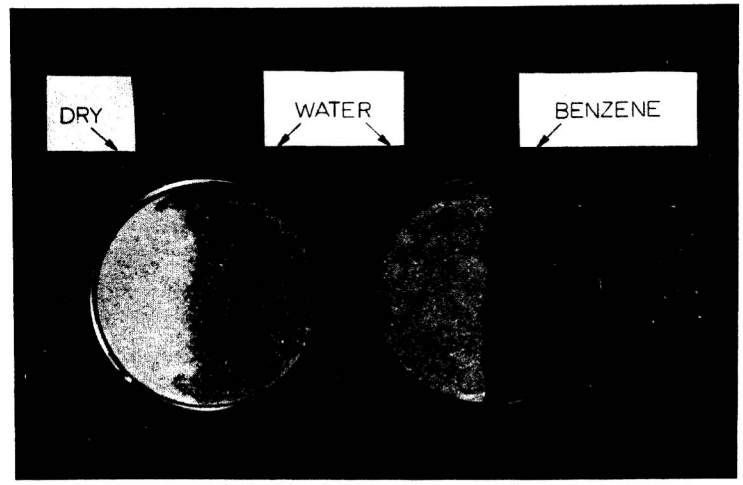

Figure 15.2 **Aquarium sand wetted with water and with benzene.**

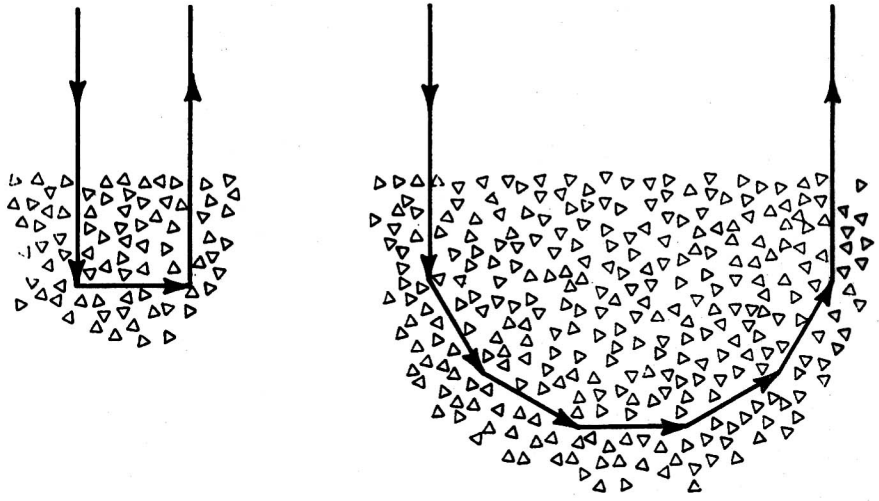

Figure 15.3 **The shortest path taken by an incident photon before re-emerging from a collection of many scatterers. On the left the average scattering angle is 90 degrees; on the right it is 30 degrees.**

(38)

For the Fluxes we must square the E_R, E_T, and for the transmitted Flux must weight by cosine of θ_T, θ_I because $\theta_T \neq \theta_I$:

$$T = \frac{F_T}{F_I} = \frac{\epsilon_2 c_2}{\epsilon_1 c_1} \frac{\cos\theta_T}{\cos\theta_I} \left(\frac{E_T}{E_I}\right)^2$$

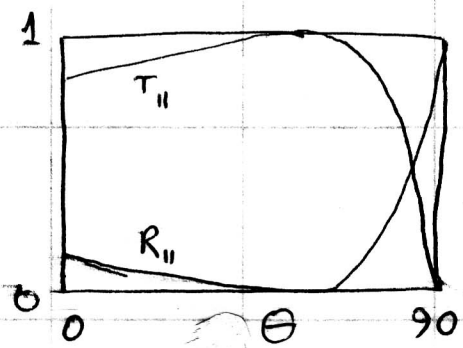

for $M = 1.5$

BOHREN & HUFFMAN

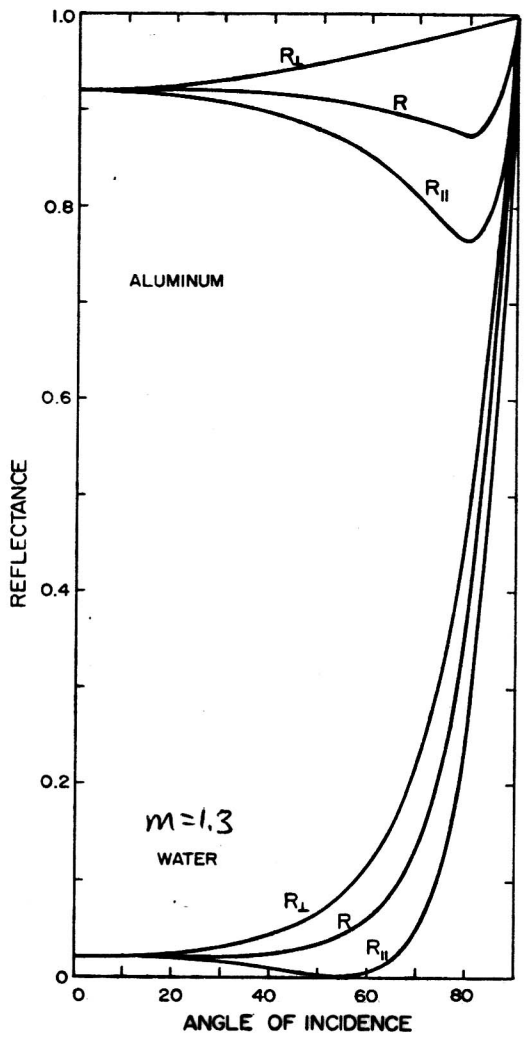

Figure 2.6 Reflectances for electric vector parallel ($R_{\parallel}$) and perpendicular ($R_\perp$) to the plane of incidence. R is the reflectance for unpolarized incident light.

3. <u>normal incidence, $\sigma \neq 0$</u> "conductors"

The formulas are the same as for $\sigma = 0$ except that now m is complex $m = m_{re} - i m_{im}$

$$R = \left|\frac{m-1}{m+1}\right|^2 = \frac{(m_{re}-1)^2 + m_{im}^2}{(m_{re}+1)^2 + m_{im}^2} \qquad (33)$$

Note that R can be large if

a) m_{re} large $\quad m_{re} \gg 1$

b) m_{im} large

c) $m_{re} \ll 1$, $m_{im} \ll 1$ ← This case does not occur. $m_{re} \ll 1$ only when m_{im} large.

eg.
A typical metal: silver, at visible wavelengths:

$$m_{re} \approx m_{im} \approx 30 \qquad R = 0.94$$

4. <u>oblique incidence, $\sigma \neq 0$</u>

This is the general case. The Fresnel formulas apply but m is complex. The equations in terms of m_{re}, m_{im} are complicated. They are given on pp 628-629 of Born & Wolf, 1980: <u>Principles of Optics</u> 6th Ed.

Reflection pattern of a metallic sphere (a perfect mirror) (of $r \gg \lambda$)

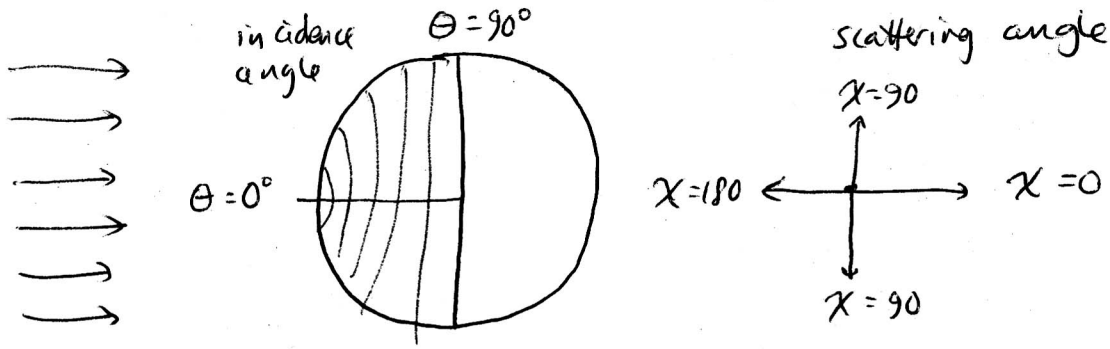

Projection of incident beam onto surface $\sim \cos\theta$

Area of zone $d\theta \sim \sin\theta$

Flux incident on a zone $d\theta$: $F_i \propto \cos\theta \sin\theta$

Reflected flux $F_r = F_i$

Scattering from incident angle θ goes into scattering-angle $\chi = \pi - 2\theta$ (the mirror angle).

Scattering-angle element $d\chi$ has solid angle $2\pi \sin\chi \, d\chi$.

The reflected flux F_r is spread over this solid angle,

so reflected intensity $I(\chi) = \dfrac{F_r}{2\pi \sin\chi \, d\chi} \propto \dfrac{\cos\theta \sin\theta}{\sin\chi}$.

But $\sin\chi = \sin[\pi - 2\theta] = 2\sin\theta\cos\theta$

so I is <u>independent of χ</u>.

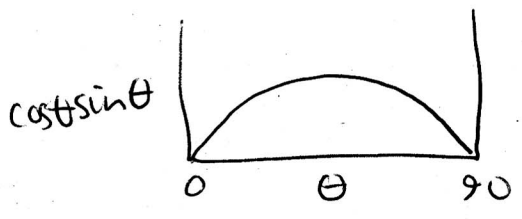

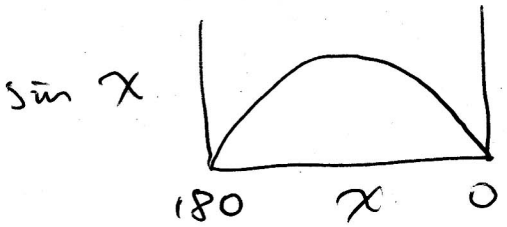

RAYLEIGH SCATTERING

Scattering of light by particles small compared to the wavelength, measured at distances far from the particle.

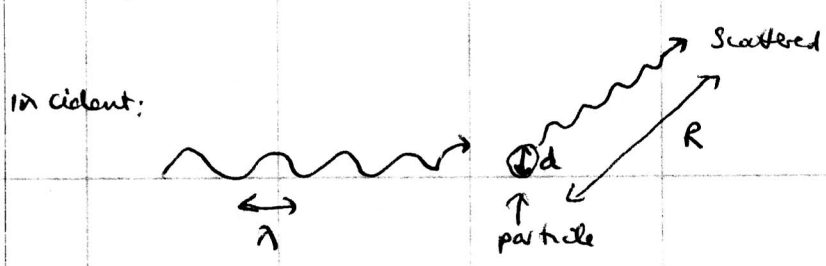

$d \ll \lambda \ll R$.

1. An accelerated charge radiates EM energy in all directions. A stationary charge does not radiate, nor does a charge at constant velocity. [e.g. Rossi, "Optics", sec. 7.6]

2. An oscillating dipole is an accelerated charge.

The dipole oscillates in a direction parallel to the incident $\bar{E}$. We observe the scattered light in any arbitrary direction. The electric field caused by the oscillating dipole contains both longitudinal and transverse components. $E_{long} \propto \frac{1}{R^2}$ $E_{trans} \propto \frac{1}{R}$

so at large R only E_{trans} remains.

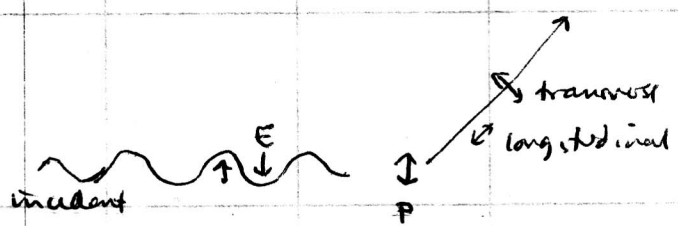

The resulting field $\bar{E}(R,t)$ is proportional to the acceleration $\bar{a}$ perpendicular to the line of sight, at time $t - R/c$

The requirement $d \ll \lambda$ is to get the same phase of the incident wave over the whole particle. The requirement $R \gg \lambda$ is to get the transverse wave only.

3. Frequency-dependence of radiated power.

$\bar{E} \propto \bar{a}$ and $\bar{a}$ is related to the dipole moment $\bar{p}$

($\bar{a}$: acceleration)

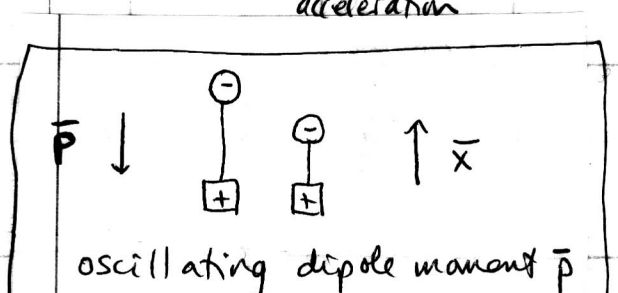

$\bar{x}$ varies in time, causing $\bar{p}$ to vary in time. Charge is e for one electron.

$$\bar{p} = -e\bar{x}$$

$$\bar{a} = \frac{d^2\bar{x}}{dt^2} \quad ; \quad -e\bar{a} = -e\frac{d^2\bar{x}}{dt^2} = \frac{d^2\bar{p}}{dt^2}$$

$\bar{p} = \bar{p}_0 \cos(\omega t + \phi)$ where ω is angular frequency of incident wave.

$$\frac{d^2\bar{p}}{dt^2} = -\omega^2\bar{p} \quad . \quad \text{so} \quad e\bar{a} = \omega^2\bar{p}$$

$$\text{so} \quad \bar{E} \propto \omega^2$$

The power radiated is proportional to $|E|^2$:

$$I \propto |E|^2 \propto \omega^4 \propto \frac{1}{\lambda^4}$$

4. Rayleigh's argument for λ-dependence considering only the dimensions.

The scattered radiation I should be proportional to I_0 and the proportionality should be some function of the variables which could possibly be relevant:

V	volume of particle
R	distance of detector from particle
λ	wavelength
c	speed of light
m_1	refractive index of medium
m_2	refractive index of particle

so $I = f(V, R, \lambda, c, m_1, m_2)\ I_0$

and f must be dimensionless.

a) A dipole radiates energy into 3 dimensions so $I \propto \frac{1}{R^2}$ for conservation of energy.

b) For a given incident field $\bar{E}$, the total dipole moment of the particle $\bar{p}$ is proportional to the volume of the particle (provided that the whole particle sees the same phase of $\bar{E}$)

The radiated $\bar{E} \propto \bar{p}$ so $\bar{E} \propto V$ and $I \propto V^2$

c) m_1 and m_2 are dimensionless. c is a velocity which cannot cancel any other variables so must not enter f.

d) To make f dimensionless, therefore, the wavelength dependence must be λ^{-4} so

$$I \propto \frac{V^2}{R^2 \lambda^4} I_0 \qquad \text{with units } \frac{m^6}{m^2 m^4}$$

5. Angular dependence : dependence of $\bar{E}$ on scattering angle Θ

(a) light polarized in the plane of scattering, $E_{\parallel}$

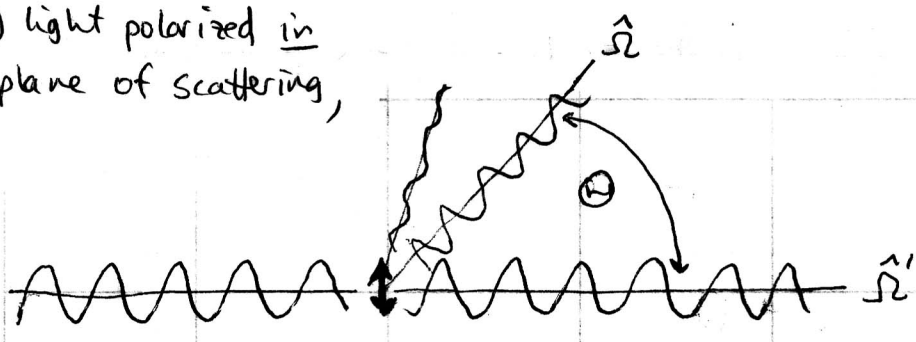

The amplitude of scattered $\bar{E}$ is proportional to $\bar{a}$ perpendicular to the line of sight $\quad \bar{a} \propto \omega^2 \bar{p}$.

let $p_{\parallel}$ be the component of $\bar{p}$ parallel to $\bar{E}_{scattered}$

$$\bar{E}_{\parallel}\ (\text{scattered}) \propto \omega^2 p_{\parallel}$$

$$p_{\parallel} = p_0 \cos\theta$$

so $\bar{E}_{\parallel} \propto \omega^2 p_0 \cos\theta$ (34)

b) light polarized perpendicular to plane of scattering $E_\perp$

The acceleration $\bar{a}$ perpendicular to the line of sight is independent of θ, so

$p_\perp = p_0$ at all angles

so $\bar{E}_\perp\ (\text{scattered}) \propto \omega^2 p_0$ (35)

c) unpolarized light

Specify the plane of scattering, then resolve the incident $\bar{E}$ into $\perp$, $\parallel$ components. They will be equal for unpolarized light.

$I_\perp\ (\text{scat}) \propto E_\perp^2$ let A be a proportionality coeff.

$I_\perp\ (\text{scat}) = A\omega^4 p_0^2$

$I_{\parallel}\ (\text{scat}) = A\omega^4 p_0^2 \cos^2\theta$

so $I\ (\text{scat}) = I_\perp + I_{\parallel} \simeq A\omega^4 p_0^2 \underbrace{(1+\cos^2\theta)}$

This is the Rayleigh phase function (needs to be normalized)

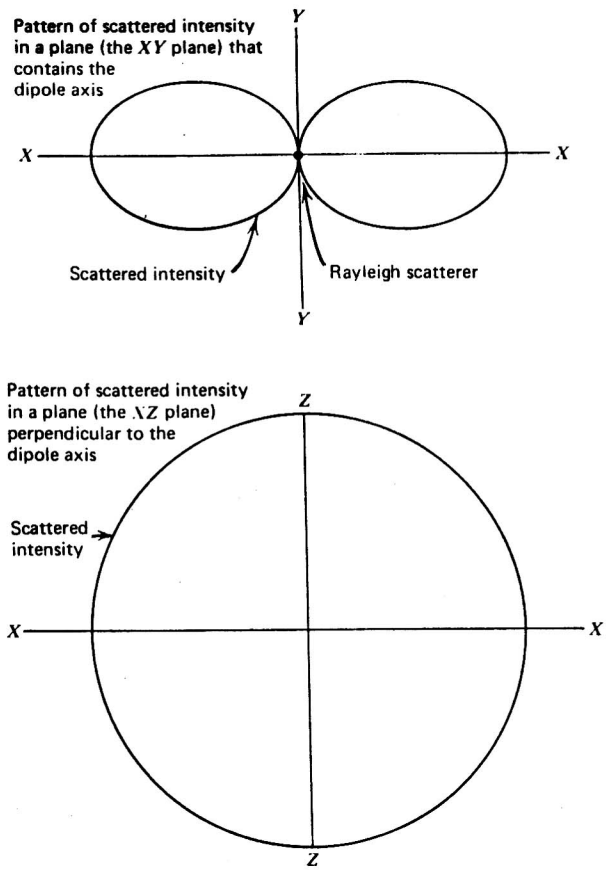

Figure 4.4 Patterns of scattered intensity for polarized incident light.

Mc Cartney

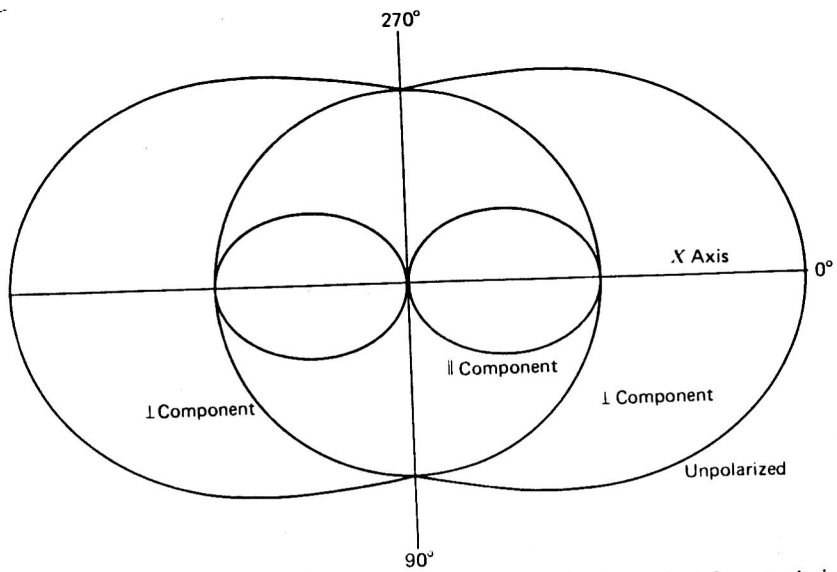

Figure 4.6 Patterns of scattered intensity, in the plane of observation, for unpolarized incident light.

Mc Cartney

6. Polarization of Sky-light

Solar beam is unpolarized. Maximum polarization of skylight is at 90° from sun

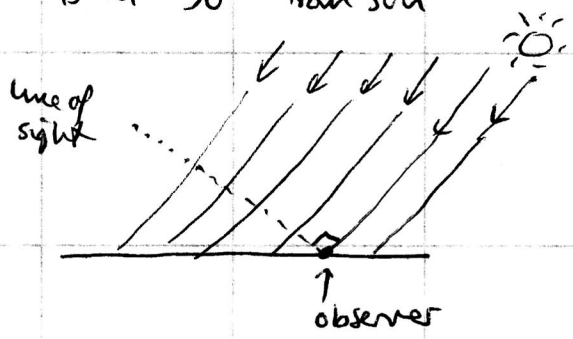

At 90° from sun, $E_{\parallel}$ is not scattered at all, but $E_{\perp}$ is scattered, so skylight is polarized.

(why isn't it completely polarized when you do this experiment?)

(7.) Rayleigh scattering in liquids and solids?

Yes, but only a small amount because the molecules are not free to oscillate independently and their spacing is rather regular. The scattered waves mostly interfere destructively.

(8.) Other approaches to Rayleigh Scattering (Young, Physics Today Jan 1982).

(a) Air has a refractive index which is a function of density. Light scatters on fluctuations in refractive index. [These relative fluctuations are small for liquids and solids.] The result is the same <u>as if</u> the molecules scattered independently (see Young, 1982).

(b) Mie scattering of EM radiation by a homogeneous sphere, in the limit of small size: $r \ll \lambda$ or $x \ll 1$ where

$$x = \frac{2\pi r}{\lambda}$$

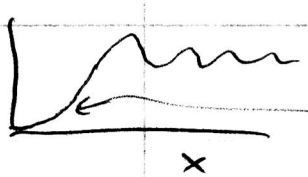

$$Q_{scat} \propto x^4 = \frac{(2\pi r)^4}{\lambda^4}$$

at small x

Valid for $x \lesssim 0.2$ but not bad up to $x \approx 1$ see next page.

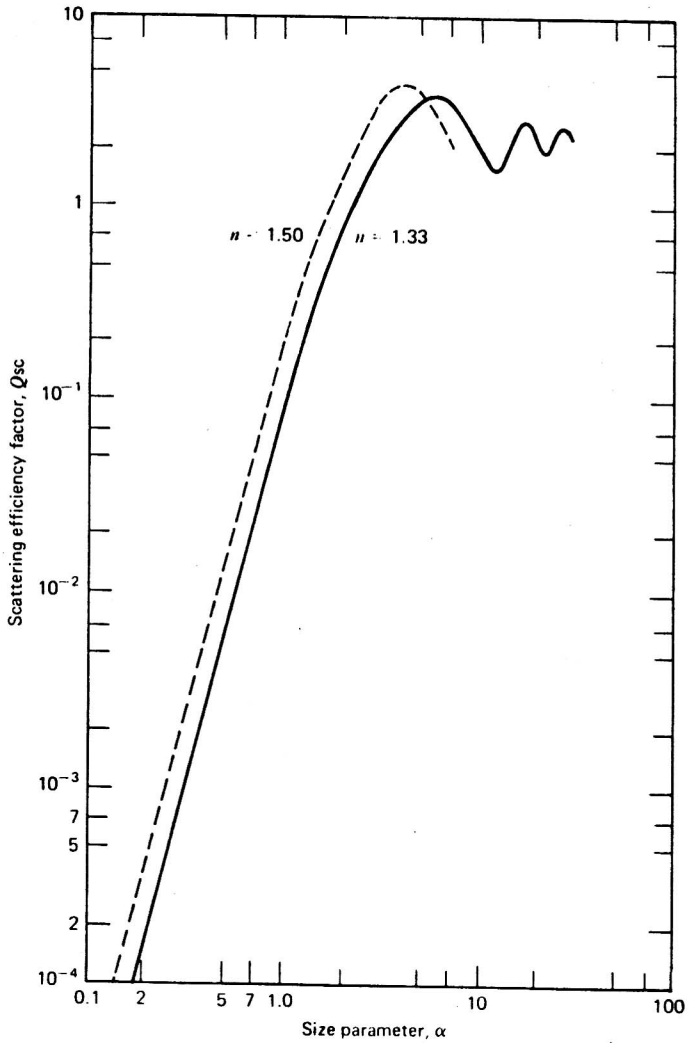

Figure 5.8 Log–log plot of scattering efficiency factor versus size parameter for two refractive indices. Data from Penndorf (1957c).

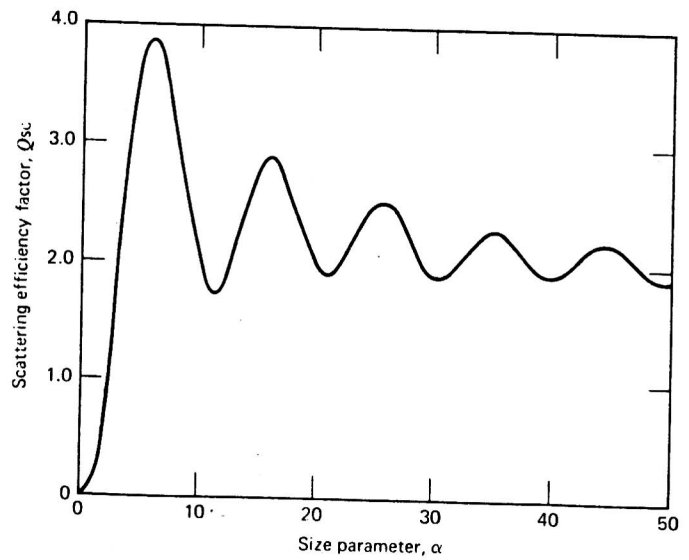

Figure 5.7 Scattering efficiency factor versus size parameter for water droplets. From List (1966).

So in the Rayleigh limit

$$Q_{scat} \propto \left(\frac{2\pi r}{\lambda}\right)^4 \propto r^4 \text{ at a particular wavelength.}$$

and the scattering cross-section C_{scat}

$$C_{scat} = \pi r^2 Q_{scat} \propto r^6 \text{ at a particular wavelength.}$$

9. Quantitative values of Rayleigh scattering

$\bar{P}$ is proportional to incident $\bar{E}$ given by the atomic polarizability α

Amplitude $p_0 = \alpha E_0$

α can be related to the bulk macroscopic refractive index m by the Clausius Mosotti equation (Lorenz-Lorentz eqn.)

$$\alpha = \frac{3\epsilon_0}{N}\left(\frac{m^2-1}{m^2+2}\right)$$ where N is number-density of molecules

Ref: Liou Appendix D
Griffith Intro to Electrodynamics pp 170-172.

Result: [Tables in McCartney Appendix H, I] "Optics of the Atmosphere"
a) for air at STP, λ = visible ($m = 1.000293$)

λ (μm)	σ_{scat}
0.3	0.145 km^{-1}
0.7	0.004 km^{-1}

b) Total optical depth of earth's atmosphere for Rayleigh scattering

λ (μm) →	0.2	0.3	0.4	0.6	0.8	1.0
τ^* →	7.63	1.22	0.363	0.0688	0.0215	0.0087

so the sky looks black in the red and near IR (except near horizon).

Kerker 1969

The remaining coefficients are proportional to still higher powers of α. Obviously when both α and m are sufficiently small, the term containing a_1 becomes the leading term in the expressions for the amplitude functions [(3.3.56), (3.3.57)]. With

$$\pi_1(\cos\theta) = 1 \tag{3.9.6}$$

and

$$\tau_1(\cos\theta) = \cos\theta \tag{3.9.7}$$

the Rayleigh formula

$$I_u = \frac{8\pi^4 a^6}{r^2\lambda^4}\left|\frac{m^2-1}{m^2+2}\right|^2(1+\cos^2\theta) \tag{3.9.8}$$

is obtained. This differs from (3.2.19) in that m may be complex. However, the derivation brings out a limitation placed upon Rayleigh scattering that may not have been evident earlier. Since retention of only the first term in the expansion of the Ricatti–Bessel functions requires that the arguments be small, it is necessary that both α and $m\alpha$ be small. This restriction upon m applies to both the real and imaginary parts.

3.9.1 Range of Validity of the Rayleigh Equation

Although the range of validity of the Rayleigh equation has long been given by a rough rule which states that the radius should not exceed about one-twentieth of the wavelength, a detailed, quantitative comparison of this equation with the full theory has been discussed only recently by Jaycock and Parfitt (1962) and Heller (1965). The latter analysis is based primarily upon the refractive index range $m = 1.00$ to 1.30, but it also includes some calculations of Lowan (1948) and of Gumprecht and Sliepcevich (1951a) for higher refractive indices.

The results are presented both as $\Delta\alpha$ and as $\Delta\tau$. The former is the percent error committed in calculating the size parameter α from the specific turbidity when the Rayleigh equation is used, while $\Delta\tau$ is the error in calculating the specific turbidity from a given value of α. The specific turbidity is

$$\tau/\phi = (3/4a)Q_{sca} \tag{3.9.9}$$

where ϕ is the volume of scattering material per unit volume and τ is the turbidity. The corresponding results involving the Rayleigh ratio at 90° are not appreciably different from those based on turbidity and will not be discussed here.

In Fig. 3.7, $\Delta\tau$ is plotted as a function of α for refractive indices up to 1.30. The results for $m = 1.00$ were obtained by extrapolation. For these refractive indices, the turbidity obtained from the Rayleigh equation is always too

high. We can now judge the validity of the conventional working rule in a quantitative way. For $m = 1.30$, the turbidity is in error by 2% when $a/\lambda = 0.06$ and by 5% when $a/\lambda = 0.1$. The Rayleigh equation is less accurate at smaller refractive indices so that at $m = 1.10$ the error is 2% for $a/\lambda = 0.04$ and 5% for $\alpha/\lambda = 0.06$.

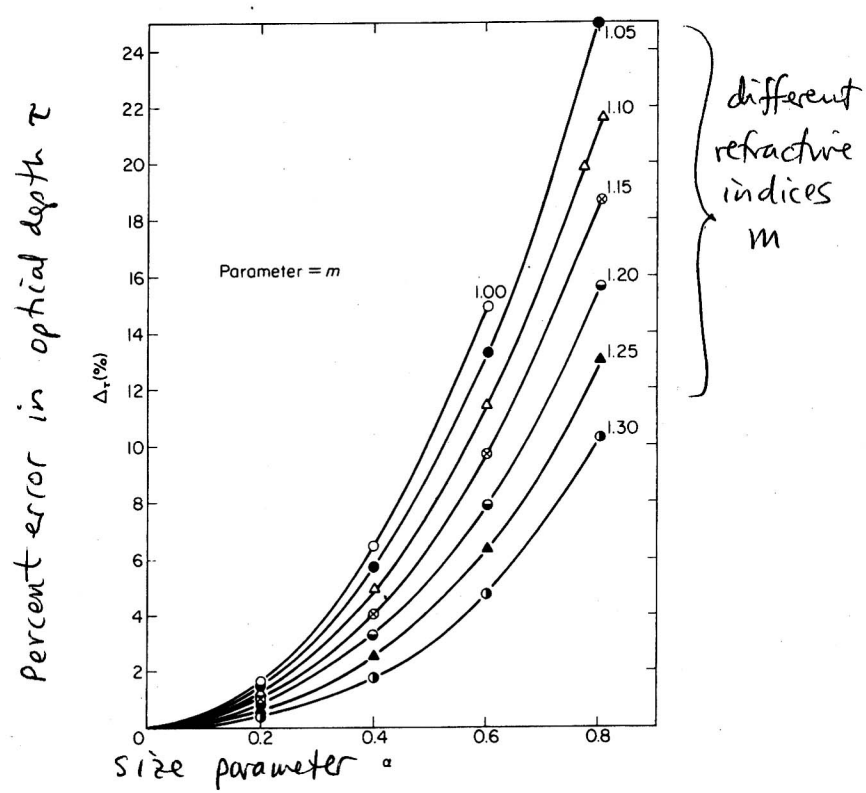

FIG. 3.7. Percentage deviation between specific turbidity calculated by the Rayleigh formula and the exact value plotted against α for $m = 1.00$ to 1.30 (Heller, 1965).

Heller has explored the decrease in $\Delta\tau$ with increasing refractive index even though he had only a limited number of computations at higher values of m available. The results are shown in Fig. 3.8 where $\Delta\tau$ is plotted against m for various values of α. The decrease of $\Delta\tau$ with m continues until there is a crossover ($\Delta\tau = 0$) to negative values. With further increase of m, $\Delta\tau$ goes through a minimum and then rises sharply through a second crossover. Between these two crossover points is a region where the size parameter is relatively high and yet the Rayleigh equation is quite accurate. Heller has

50

Mie Theory — Gustav Mie (1908)

references: [van de Hulst; Bohren & Huffman; Hansen & Travis] — 1974

Scattering of a plane EM wave by a homogeneous sphere of radius a (size parameter $x = \frac{2\pi a}{\lambda}$), with complex refractive index m_1, in medium of complex refractive index m_2, so that relative refractive index is $m = \frac{m_1}{m_2}$.

Limiting cases

1. geometric optics: surface is locally plane. ($x \gg 1$)
2. Rayleigh: whole particle sees same phase ($x \ll 1$)
3. Mie: the general solution for any x

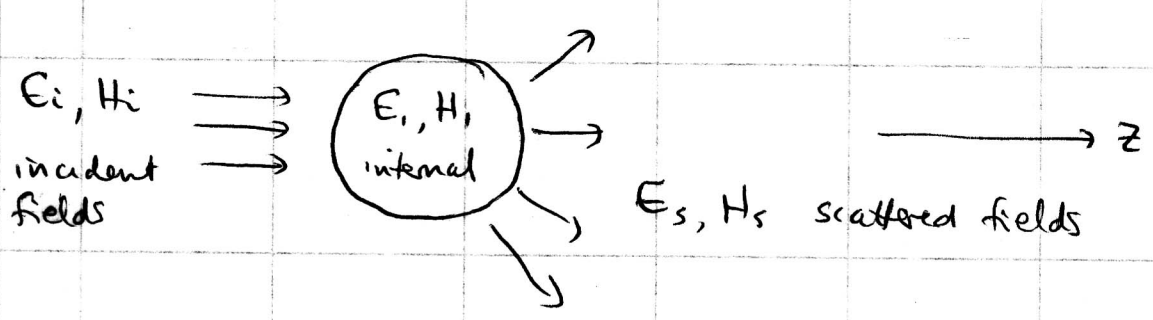

medium 1 is inside the particle
medium 2 is the surroundings.

$E_s \Rightarrow H_s$, so we need only compute E_s.

What we can measure is $\bar{I}$, the 4 components of the Stokes vector, as functions of Θ:

$$\begin{pmatrix} I_s(\Theta) \\ Q_s(\Theta) \\ U_s(\Theta) \\ V_s(\Theta) \end{pmatrix} = \frac{\tilde{\omega} C_{ext}}{4\pi r^2} \begin{pmatrix} & \underline{\underline{P}}(\Theta) & \end{pmatrix} \begin{pmatrix} I_i \\ Q_i \\ U_i \\ V_i \end{pmatrix}$$

The phase matrix has 16 components but they are not all independent. To compute $\bar{I}_s$ we need only E_l^s and E_r^s:

$$\begin{pmatrix} E_l^s \\ E_r^s \end{pmatrix} = \frac{1}{ikr} e^{(ikr - ikz)} \begin{pmatrix} S_2 & S_3 \\ S_4 & S_1 \end{pmatrix} \begin{pmatrix} E_l^i \\ E_r^i \end{pmatrix}$$

E_l, E_r are complex (include phase) so S_i are complex.
So there are only 8 numbers not 16 to be determined
Actually only 7: 4 $|S_i|$ and 3 phase differences
r is distance from particle.

The factor $\frac{1}{r}$ gives falloff of E with $\frac{1}{r}$

The $\frac{1}{ik}$ factor is for convenience, so that S_i will be dimensionless.

(Recall $k = \frac{2\pi}{\lambda}$, so $k \cdot r$ is dimensionless)

$e^{ik(r-z)}$ is the phase difference at a particular time between the incident wave continuing along z and the scattered wave at distance r

For spherical particles $S_3 = S_4 = 0$ so we need $S_1(\theta), S_2(\theta)$ only.

$\{S\}$ is called the "amplitude scattering matrix"

Outline of procedure.

incident wave E_i, H_i

wave inside particle E_1, H_1

scattered wave E_s, H_s

wave outside particle $E_2 = E_s + E_i$

$H_2 = H_s + H_i$

These waves must obey Maxwell's equations.

A solution must satisfy 4 boundary conditions (used earlier to get Fresnel's laws)

$(B_2 - B_1) \cdot n = 0$

$(D_2 - D_1) \cdot n =$ surface charge density $= 0$

Tangential components of E & H are continuous across the boundary.

$(E_2 - E_1) \times n = 0$

$(H_2 - H_1) \times n =$ surface current density $= 0$

where n is normal to surface

a) choose a plane of scattering

b) resolve incident wave into $E_\perp$, $E_\parallel$

c) Relate the EM vector wave eqn to a scalar wave eqn satisfied by a function ψ such that if ψ is known E can be obtained.

$$\nabla^2\psi + k^2\psi = 0. \qquad \psi \text{ is the "generating function".} \qquad (36)$$

d) Solve (36) by separation of variables

$$\psi = R(r)\,\Theta(\theta)\,\Phi(\phi)$$

Use spherical coordinates. Origin at center of sphere

e) Plane EM wave is expanded in infinite series.

The functions R, Θ are series.
(Spherical Bessel functions, Associated Legendre functions)

f) Boundary conditions at surface of sphere match E_2 to E_1, and determine coefficients of terms in the solution R, Θ, Φ.

** g) Solution depends on kr. Take limit as $kr \to \infty$ to get "far-field" solution far from particle. (transverse wave only) ** $(r \gg a)$

Result.

$$S_1(\theta) = \sum_{n=1}^{\infty} \frac{2n+1}{n(n+1)} \left[a_n \pi_n(\mu) + b_n \tau_n(\mu)\right]$$

$$S_2(\theta) = \sum_{n=1}^{\infty} \frac{2n+1}{n(n+1)} \left[b_n \pi_n(\mu) + a_n \tau_n(\mu)\right] \qquad (37)$$

where $\mu = \cos\theta$

a_n, b_n, τ_n and π_n are functions.

τ_n and π_n give the θ-dependence. They are related to Legendre polynomials $P_n(\mu)$; they depend only on θ

a_n and b_n are functions of (x, m) where $m = m_{re} - i\, m_{im} = \frac{m_1}{m_2}$

a_n and b_n are related to Bessel functions.

The sum in (37) does not have to go to ∞ because $a_n, b_n \to 0$ for $n > x$.

Functions $\tau_n(\mu)$, $\pi_n(\mu)$:

$$\pi_n(\mu) = \frac{dP_n(\mu)}{d\mu} \quad \text{and} \quad \tau_n(\mu) = \mu\,\pi_n(\mu) - (1-\mu^2)\frac{d\pi_n(\mu)}{d\mu}$$

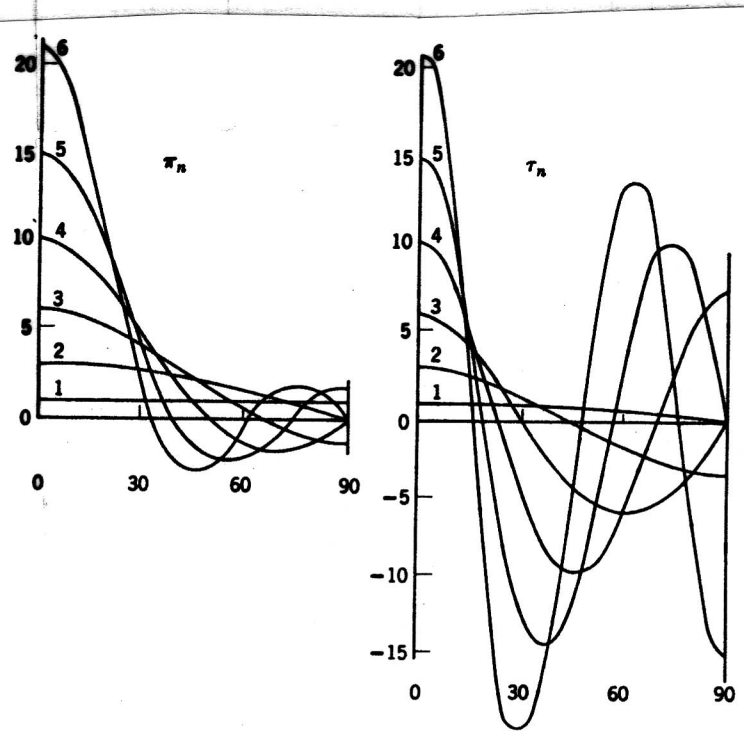

Fig. 18. The two sets of functions of the scattering angle θ, which occur in the Mie formulae, for $n = 1$ to 6.

van de Hulst p. 125.

Bohren & Huffman (56)

noted previously, **M** has no radial component, and for sufficiently large kr the radial component of **N** for the scattered field is negligible compared with the transverse component.

We have shown in Fig. 4.2 how the functions j_n and y_n behave, and the functions $\sin\phi$, $\cos\phi$ are well known. Thus, it only remains for us to show the behavior of the functions π_n and τ_n, which determine the θ dependence of the fields. Polar plots of π_n and τ_n for $n = 1$–5 are shown in Fig. 4.3; these plots are more pleasing to the eye if we allow θ to range from 0 to 360°. Note

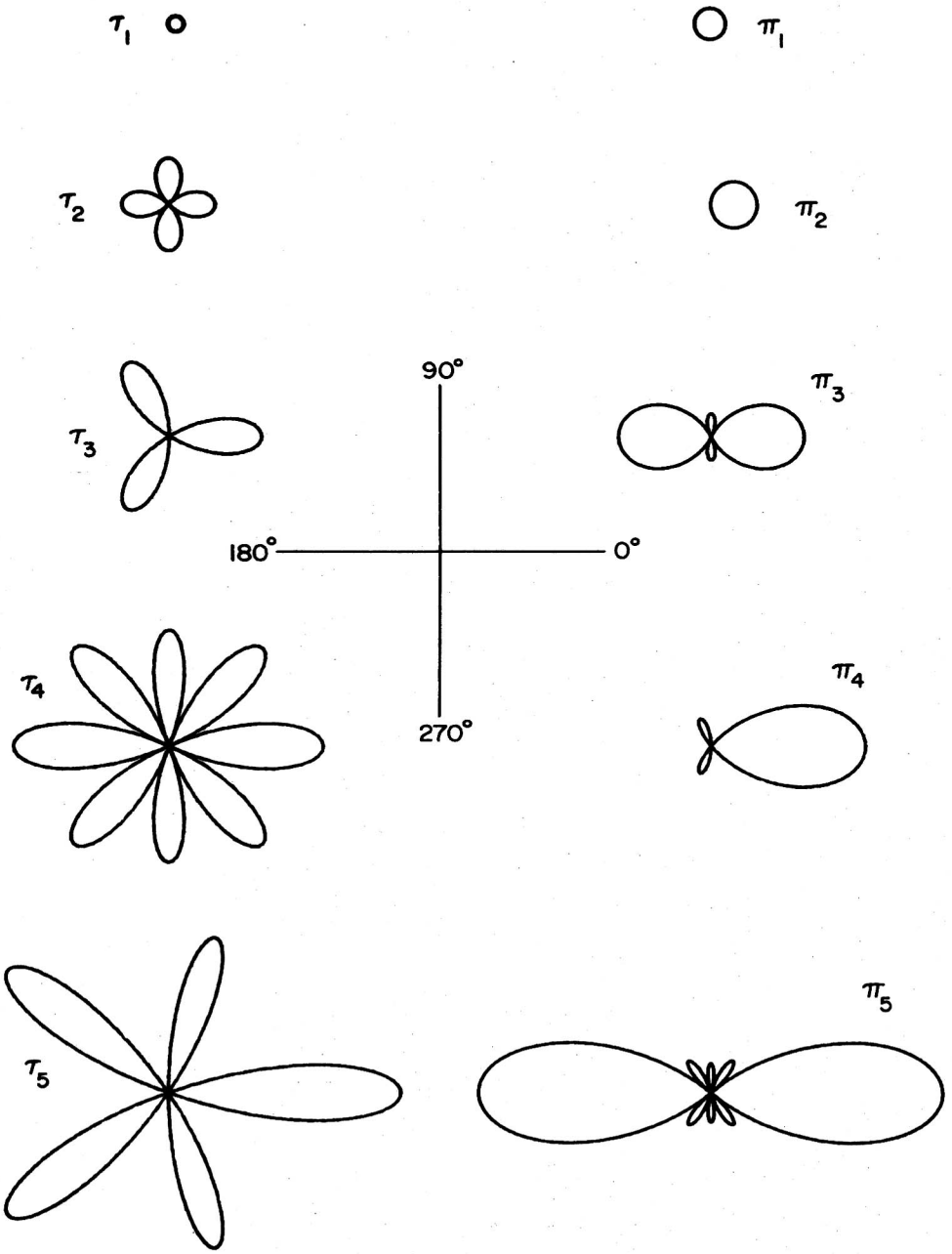

Figure 4.3 Polar plots of the first five angle-dependent functions π_n and τ_n. Both functions are plotted to the same scale.

coefficient-functions $a_n(m,x)$ and $b_n(m,x)$:

$m = \frac{m_1}{m_2}$

$$a_n = \frac{\psi_n(x)\,\psi_n'(mx) - m\,\psi_n(mx)\,\psi_n'(x)}{\xi_n(x)\,\psi_n'(mx) - m\,\psi_n(mx)\,\xi_n'(x)}$$

$$b_n = \frac{m\,\psi_n(x)\,\psi_n'(mx) - \psi_n(mx)\,\psi_n'(x)}{m\,\xi_n(x)\,\psi_n'(mx) - \psi_n(mx)\,\xi_n'(x)}$$

note that $a_n = b_n = 0$ if $m = 1$

$\left[\psi_n'(x) \text{ means } \frac{d\psi_n(x)}{dx}\right]$

where ψ and ξ are modified spherical Bessel functions called "Ricatti-Bessel functions" : (not to be confused with the generating function ψ)

$$\psi_n(x) = x\,j_n(x)$$

$$\xi_n(x) = \psi_n(x) - i\,x\,y_n(x)$$

where j_n and y_n are related to the cylindrical Bessel functions by

$$j_n(x) = \sqrt{\frac{\pi}{2x}}\; J_{n+\frac{1}{2}}(x)$$

$$y_n(x) = \sqrt{\frac{\pi}{2x}}\; Y_{n+\frac{1}{2}}(x)$$

plotted by Bohren & Huffman on next page.

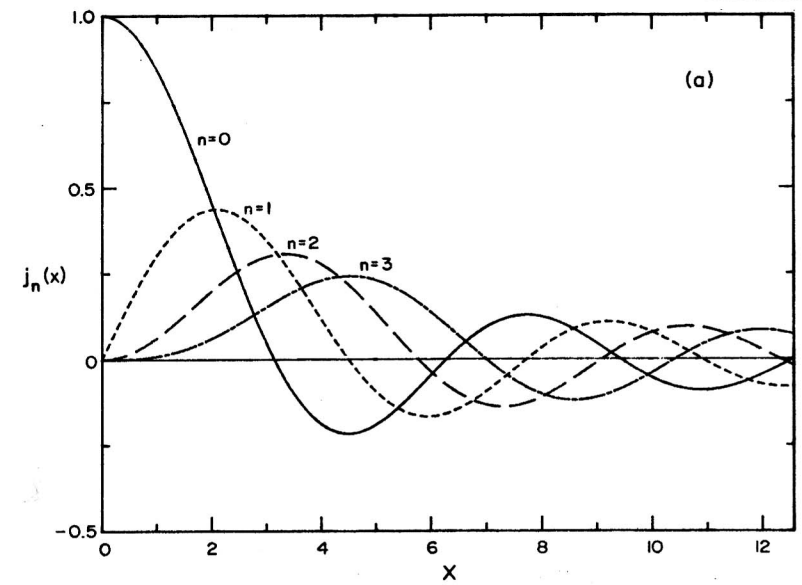

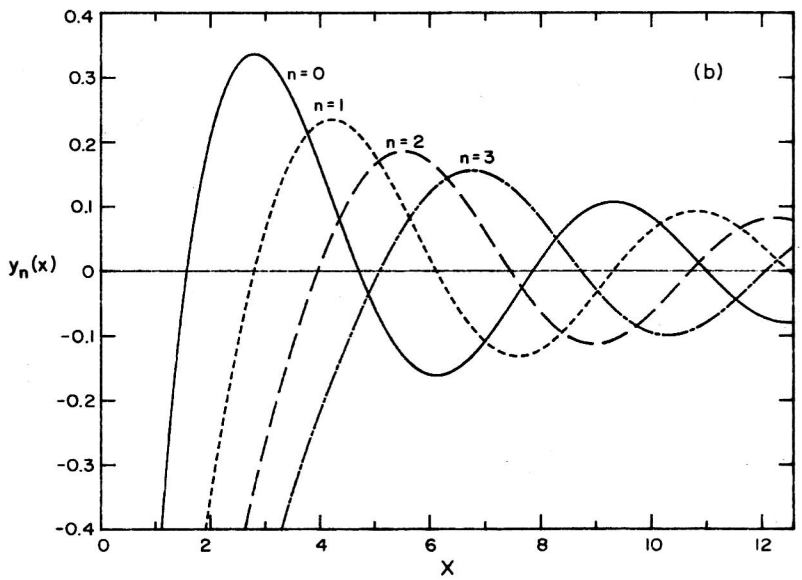

Figure 4.2 Spherical Bessel functions of the first (*a*) and second (*b*) kind.

BOHREN & HUFFMAN p. 88.

Recursion formulas are used to compute a_n, b_n, τ_n, π_n :

$$a_{n+1} = f(a_{n-1}, a_n) \quad , \text{etc.}$$

Efficiencies are Q_{ext}, Q_{sca} and asymmetry factor g are averages over Θ

so they are functions only of a_n & b_n not τ_n, π_n.

e.g. van de Hulst shows that

$$Q_{sca} = \frac{1}{2\pi x^2} \int_{4\pi} \left[|S_1(\theta)|^2 + |S_2(\theta)|^2 \right] d\omega = \frac{2}{x^2} \sum_{n=1}^{\infty} a_n^* a_n + b_n^* b_n$$

Computation

The number of terms required is slightly more than x, using the criterion that the series can be terminated when $|a_n|^2 + |b_n|^2 < 10^{-14}$

Table 5. **The range [N_{min}, N_{max}] of the number of terms in the Mie series, as a function of size parameter x. The range was determined by varying Re(m) from 1.05 to 2.50 and Im(m) from 0 to 1 in small steps.**

from WISCOMBE, 1979 : NCAR Tech. Note 140+STR

x	$N_{min} - N_{max}$	x	$N_{min} - N_{max}$
0.1	2-3	3,000	3,052-3,058
0.3	3-3	6,000	6,068-6,074
1	5-5	8,000	8,076-8,080
3	8-9	10,000	10,081-10,087
10	18-20	12,000	12,086-12,092
33	44-47	14,000	14,090-14,097
100	117-120	16,000	16,087-16,101
333	357-362	18,000	18,094-18,105
1,000	1,038-1,041	20,000	20,102-20,108

Petty

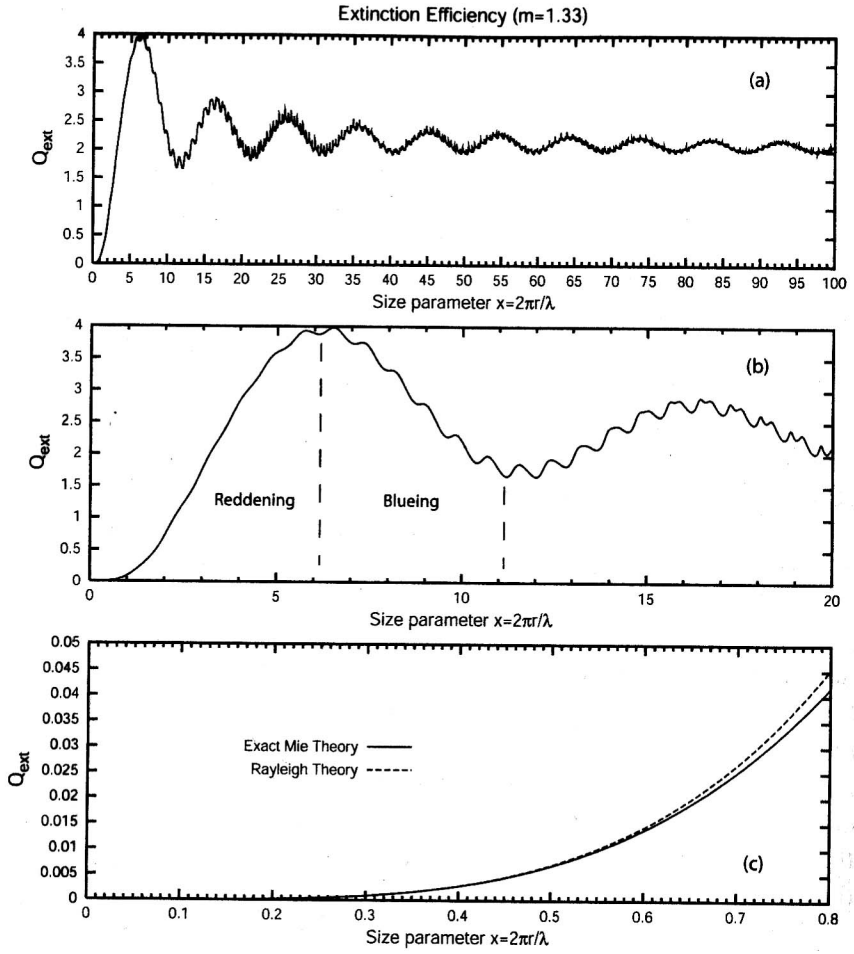

Fig. 12.4: The extinction efficiency Q_e as a function of size parameter x for a non-absorbing sphere with $m = 1.33$, for various ranges of x. (a) "Big picture" view, showing that $Q_e \to 2$ as $x \to \infty$. (b) Detail for $x < 20$, with examples of subranges for which extinction increases with x (reddening) or decreases with x (blueing). (c) Detail for $x < 0.8$, comparing the Rayleigh (small particle) approximation and exact Mie theory.

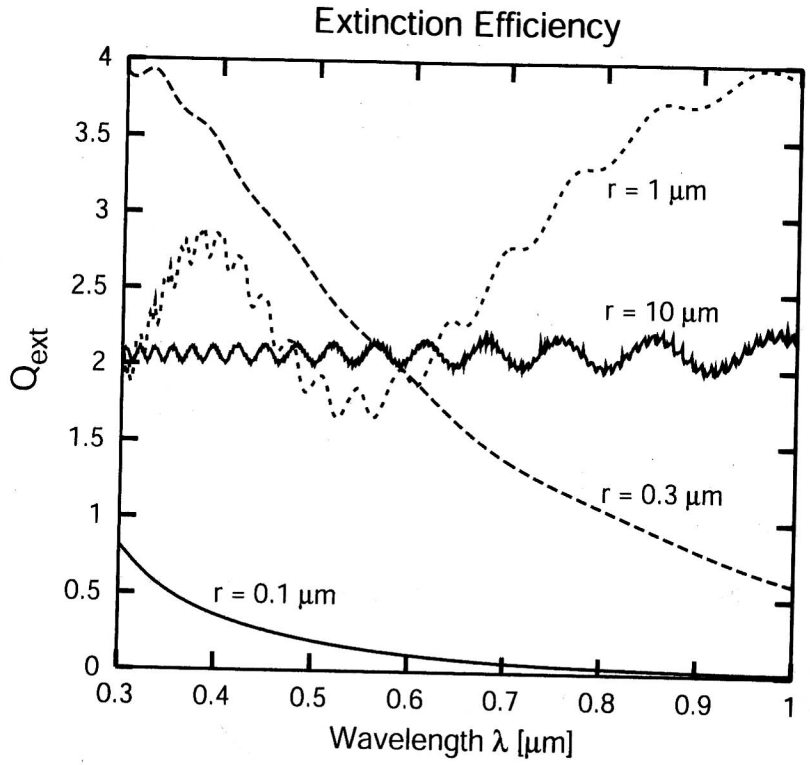

Fig. 12.5: The extinction efficiency as a function of wavelength for water droplets of the indicated sizes.

Bohren & Huffman

(61)

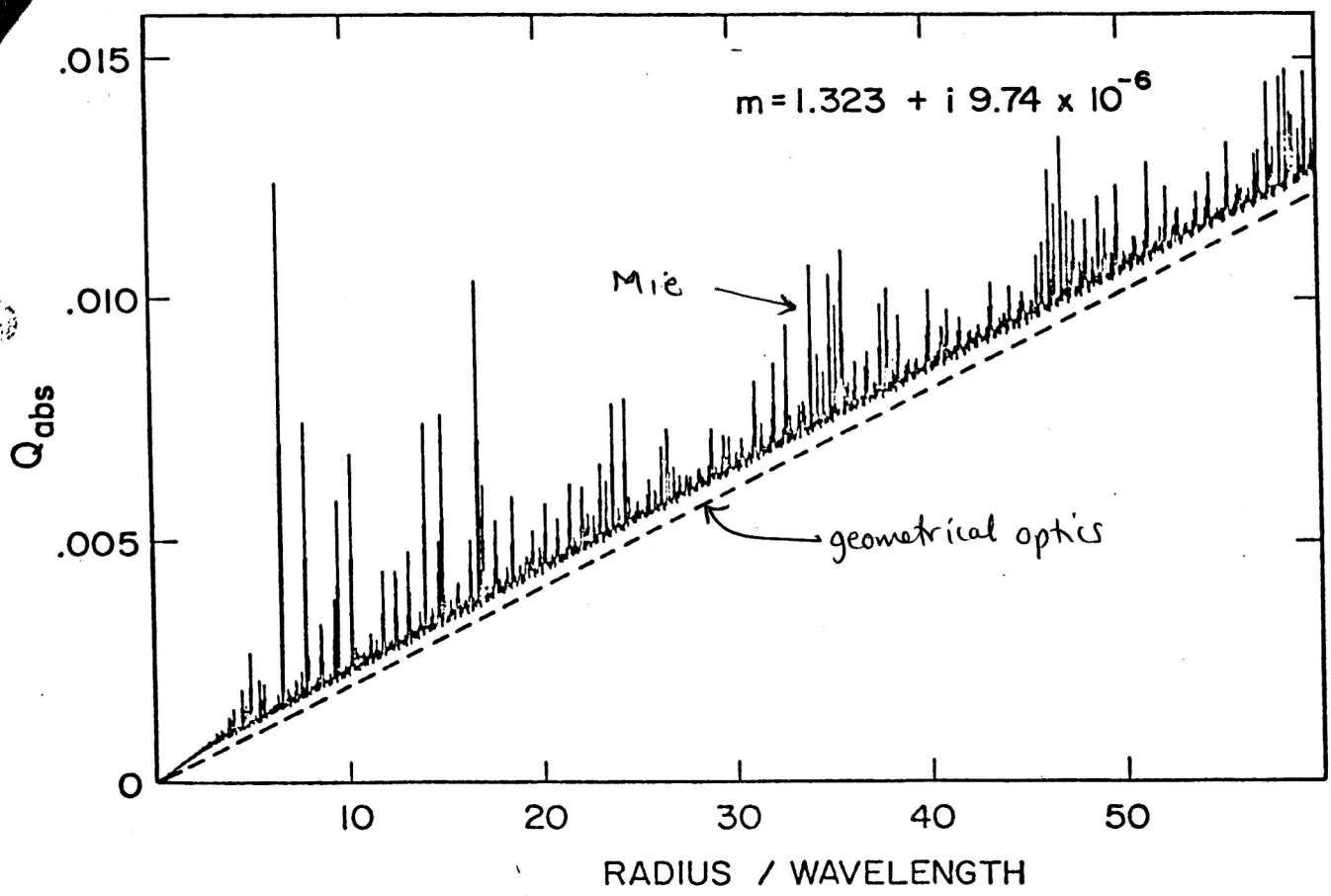

van de Hulst

only for m close to 1 but even for values of m as large as 2. This is brought out in Fig. 32, where the extinction curves for $m = 1.5$, $m = 1.33$, $m = 0.93$, $m = 0.80$, and $m \to 1$ are plotted with a common scale of ρ.

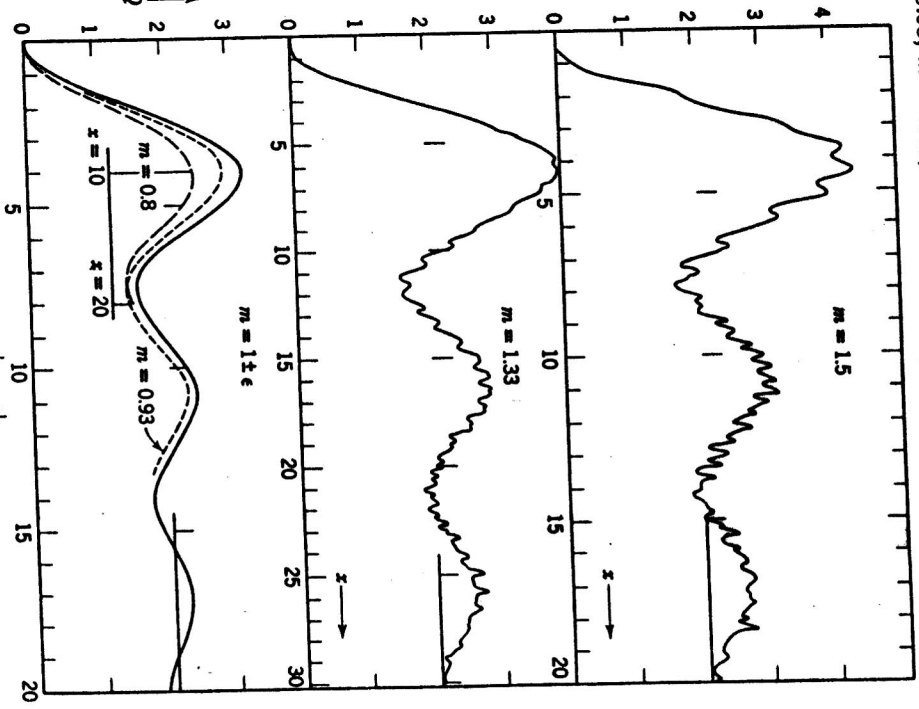

Fig. 32. Extinction curves computed from Mie's formulae for $m = 1.5$, 1.33, 0.93, and 0.8. The scales of x have been chosen in such a manner that the scale of $\rho = 2x|m - 1|$ is common to these four curves and to the extinction curve for $m = 1 \pm \varepsilon$.

The scale of ρ at the bottom holds for all five graphs. The corresponding scales of x depend on m. For $m = 1.05$ or 0.95 the range shown in the figure corresponds to the range of x from 0 to 200.

The most striking feature is the existence of a sequence of maxima and minima. The maxima occur when the term $-e^{-i\rho \sin\tau}$ enhances the term

Petty.

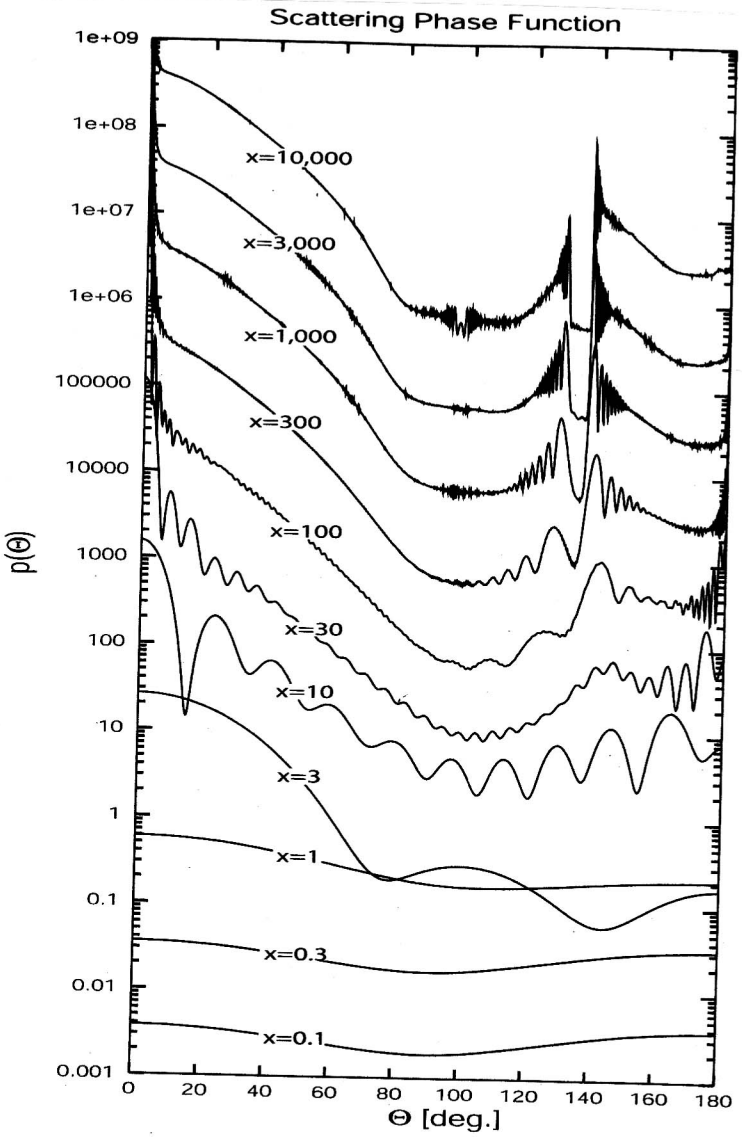

Fig. 12.7: Plots of Mie-derived phase functions $p(\Theta)$ for various values of x, assuming $m = 1.33$ (fine-scale oscillations in the curves for large x have been smoothed out by allowing x to vary over a narrow range). The vertical scale is logarithmic but otherwise arbitrary; each curve has been displaced upward from the previous one for clarity. Note increasing asymmetry and complexity of phase functions with increasing x. The topmost curve ($x = 10,000$) is very similar to that predicted by geometric optics except for the narrow forward and backward peaks at 0° and 180°. See Figs. 12.8 and 12.9 for polar plots of some of these same curves.

Space Science Reviews vol. 16. 1974

LIGHT SCATTERING IN PLANETARY ATMOSPHERES

JAMES E. HANSEN and LARRY D. TRAVIS
Goddard Institute for Space Studies, New York, N.Y. 10025, U.S.A.

(Received 15 May, 1974)

Abstract. This paper reviews scattering theory required for analysis of light reflected by planetary atmospheres. Section 1 defines the radiative quantities which are observed. Section 2 demonstrates the dependence of single-scattered radiation on the physical properties of the scatterers. Section 3 describes several methods to compute the effects of multiple scattering on the reflected light.

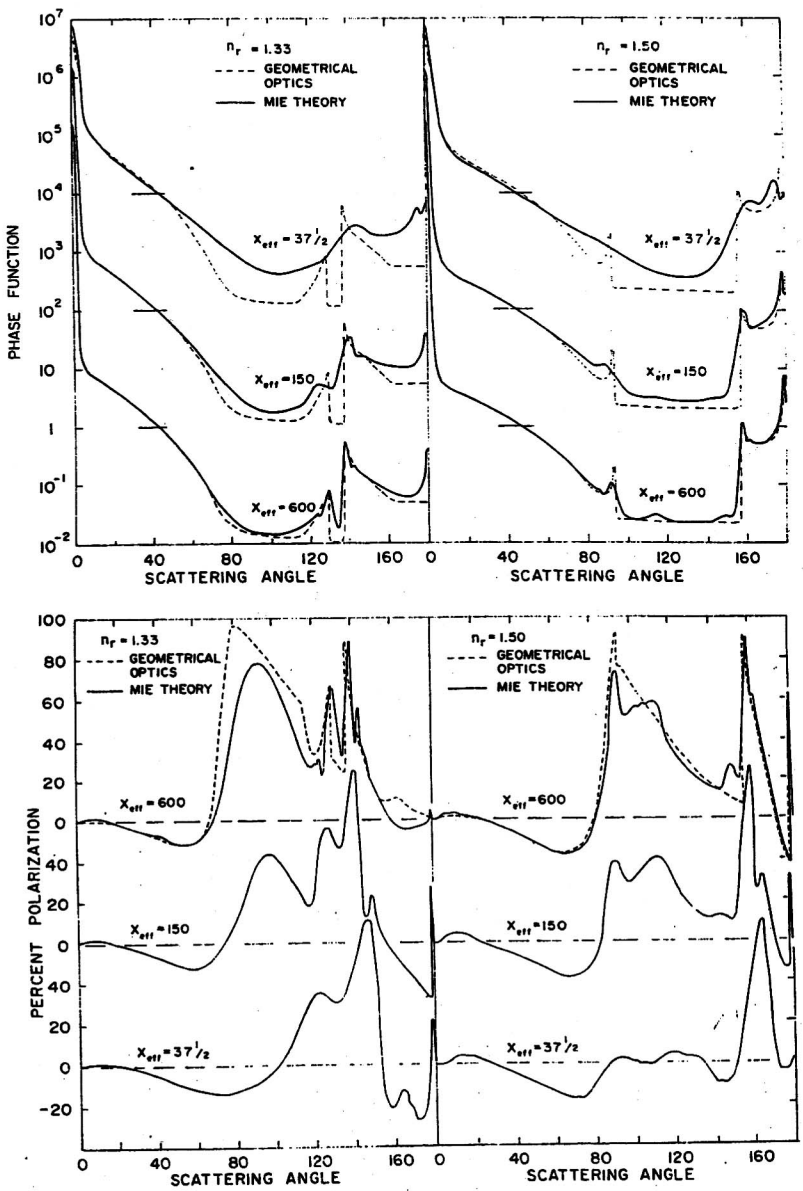

Fig. 5. Comparison of geometrical optics and Mie theory. The phase function (upper figure) and percent polarization (lower figure) are for single scattering of unpolarized light by spheres. Results are shown for two real refractive indices and three values of x_{eff}, which is the effective size parameter for the size distribution (2.11). For the phase function the scale applies to the curves for $x_{eff} = 600$, the other curves being successively displaced upward by a factor of 100.

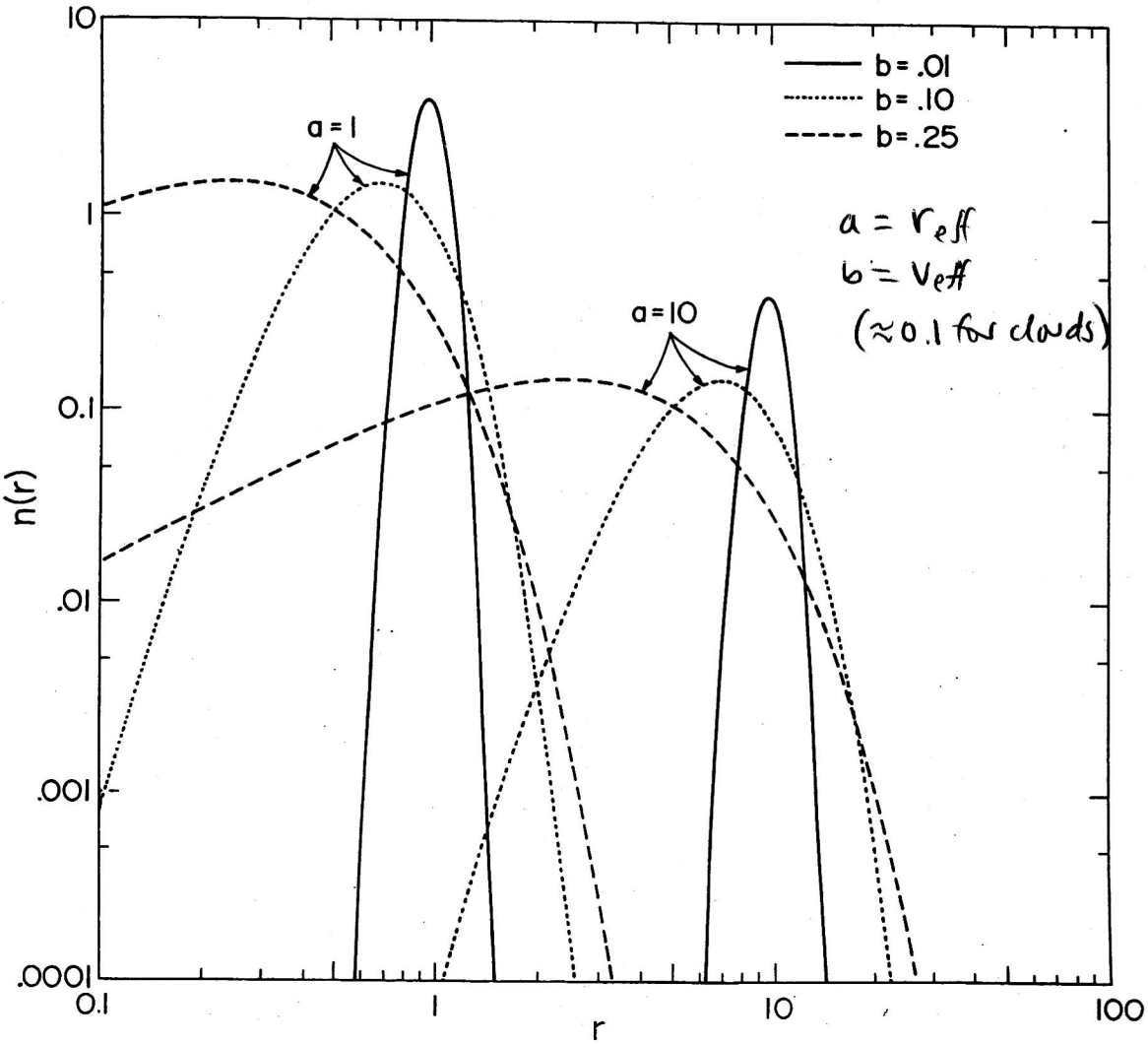

Fig. 7. Standard size distribution (2.56) for 2 values of a and three values of b. The size distribution is normalized so that the integral over all sizes is $N=1$.

The curve $b=0$ in Figure 8 gives Q_{sca} for a single particle, as a function of $x=2\pi r/\lambda$. This curve is characterized by a series of major maxima and minima of wavelength ~ 10 in x and superimposed 'ripples' of wavelength ~ 0.8 in x. The major maxima and minima are due to interference of light diffracted ($l=0$) and transmitted ($l=2$) by the particle, these two components making up $\sim 95\%$ of the scattered light (Figure 4). The phase shift for a light ray passing through the sphere along a diameter is $\varrho=2x(n_r-1)$. Thus constructive (or destructive) interference occurs successively at intervals $\sim 2\pi$ in ϱ, or ~ 9.5 in x for $n_r=1.33$. The curves of Q_{sca} for other values of n_r are qualitatively similar if graphed as a function of ϱ, as shown in Figure 32 of van de Hulst (1957).

The ripple on the Q_{sca} curve for a single particle arises from the last few significant terms in the Mie series, (2.42), as demonstrated by Bryant and Cox (1966). According to the localization principle these terms arise from edge rays, i.e., from the light rays grazing the sphere. These rays set up surface electromagnetic waves which travel around the sphere spewing off energy in all directions. Since there are focal points at

$\alpha=0°$ and $\alpha=180°$ the main effect of the surface waves is noticed in these directions. At $\alpha=180°$ the surface waves give rise to an enhanced intensity which contributes to the glory, and is the main cause of the glory for cases in which there is no contribution from geometrical optics. At $\alpha=0°$ the intensity due to surface waves is small compared to the intensity of diffracted light. However the diffracted radiation and the radiation arising from the surface waves optically interfere, causing the ripples in the extinction curve. van de Hulst (1957) and Bryant and Cox (1966) suggest different phenomenological models to explain the wavelength of the ripple. In the model of van de Hulst the surface waves are assumed to take short cuts by jumping through the sphere; in the model of Bryant and Cox it is assumed that the surface waves are only slightly damped, i.e., that they involve hundreds of circumvolutions. Numerical results presented below for absorbing spheres suggest that the model of van de Hulst may be the closer to reality.

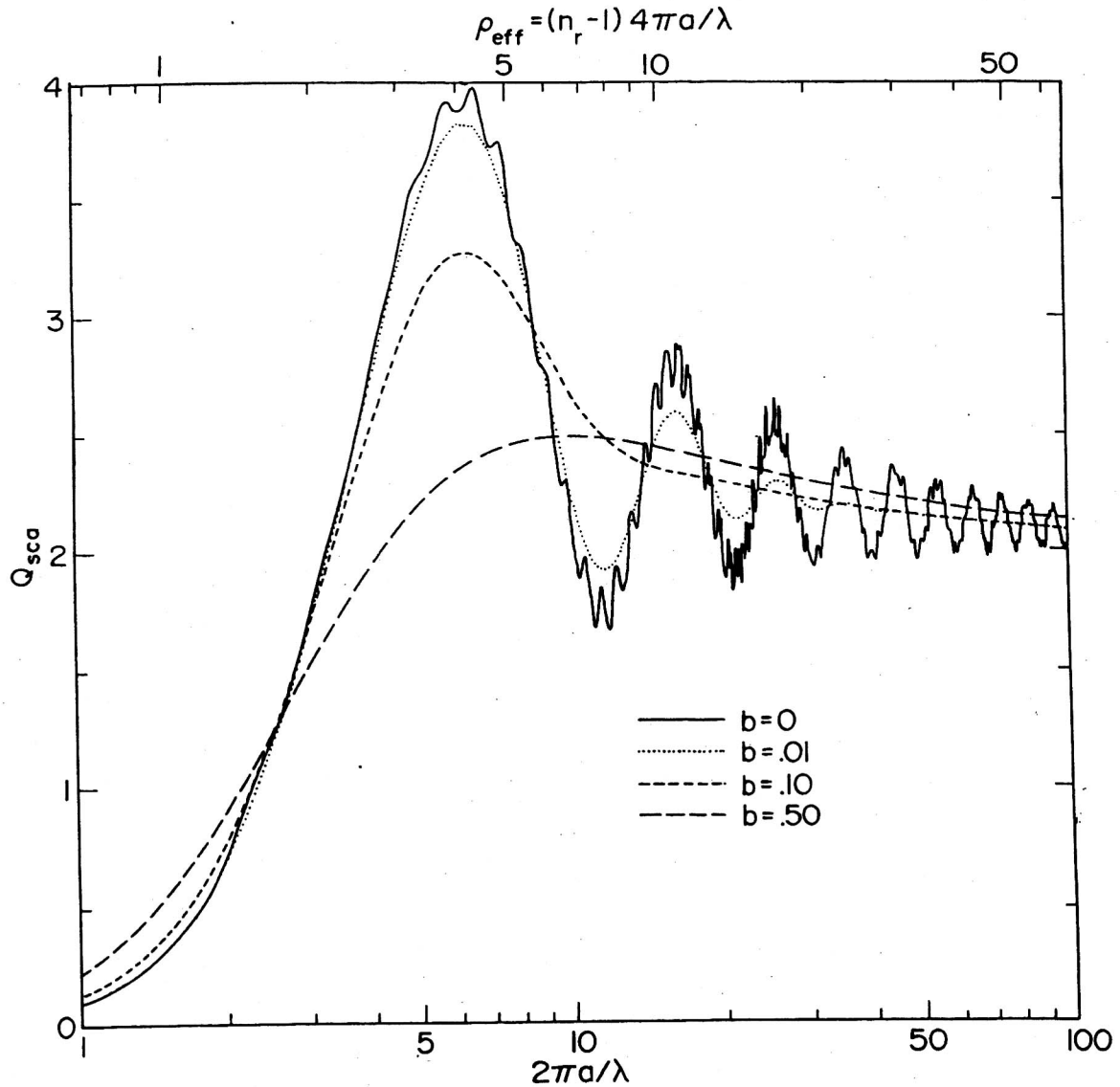

Fig. 8. Efficiency factor for scattering, Q_{sca}, as a function of the effective size parameter, $2\pi a/\lambda$. The standard size distribution (2.56) was used with four values of the effective variance b. For the case $b=0$, $2\pi a/\lambda = 2\pi r/\lambda \equiv x$. The refractive index is $n_r=1.33$, $n_i=0$.

(66)

Figure 8 demonstrates that even a small dispersion of sizes* washes out the ripple in Q_{sca}. However the first major maximum persists to large values of b, so its effect must be noticeable in many cases. One example is an increase of atmospheric extinction with increasing wavelength ('anomalous extinction') which is sometimes observed (e.g., Porch *et al.*, 1973). This must be due to extinction by atmospheric aerosols with $\varrho_{eff} \sim 5$. The magnitude of the effect can serve as a rough measure of the width of the size distribution.

Figure 9 illustrates that both the ripples and the major maxima and minima damp

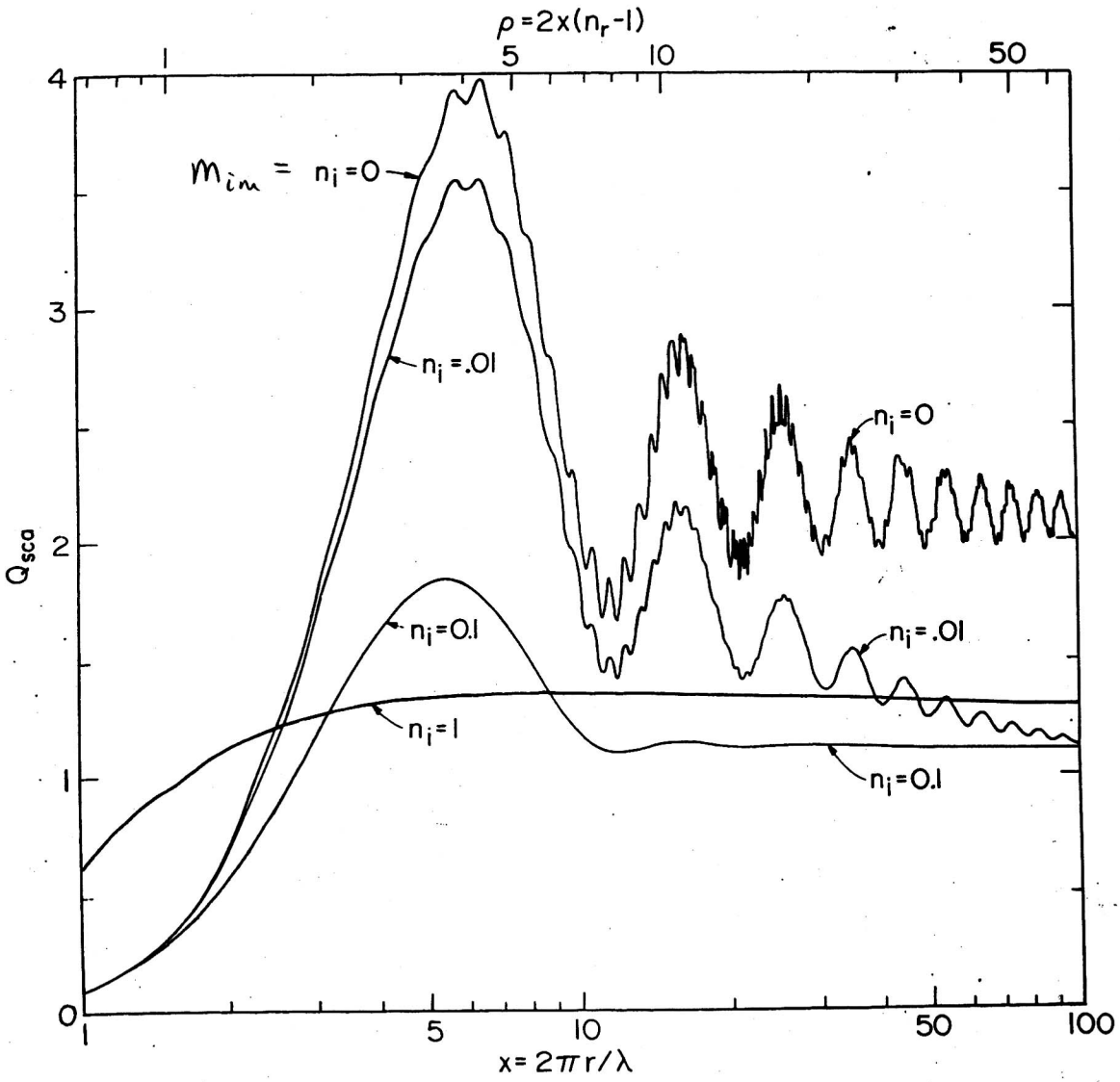

Fig. 9. Efficiency factor for scattering, Q_{sca}, as a function of the size parameter $x = 2\pi r/\lambda$. The refractive index is $n_r = 1.33$, with results shown for four values of n_i.

* v_{eff} is ~0.06–0.08 for the size distributions measured for particles in the stratosphere (the Junge layer) by Friend (1966) and Mossop (1965); it is ~0.10–0.20 for the distributions measured by Diem (1948) for water clouds, but values as large as ~0.5 were found by Weickmann and aufm Kampe (1953), whose measurements included larger particles than those sampled by Diem; v_{eff} is ~0.5–20 for the typical size distributions found by Junge (1963) for tropospheric aerosols.

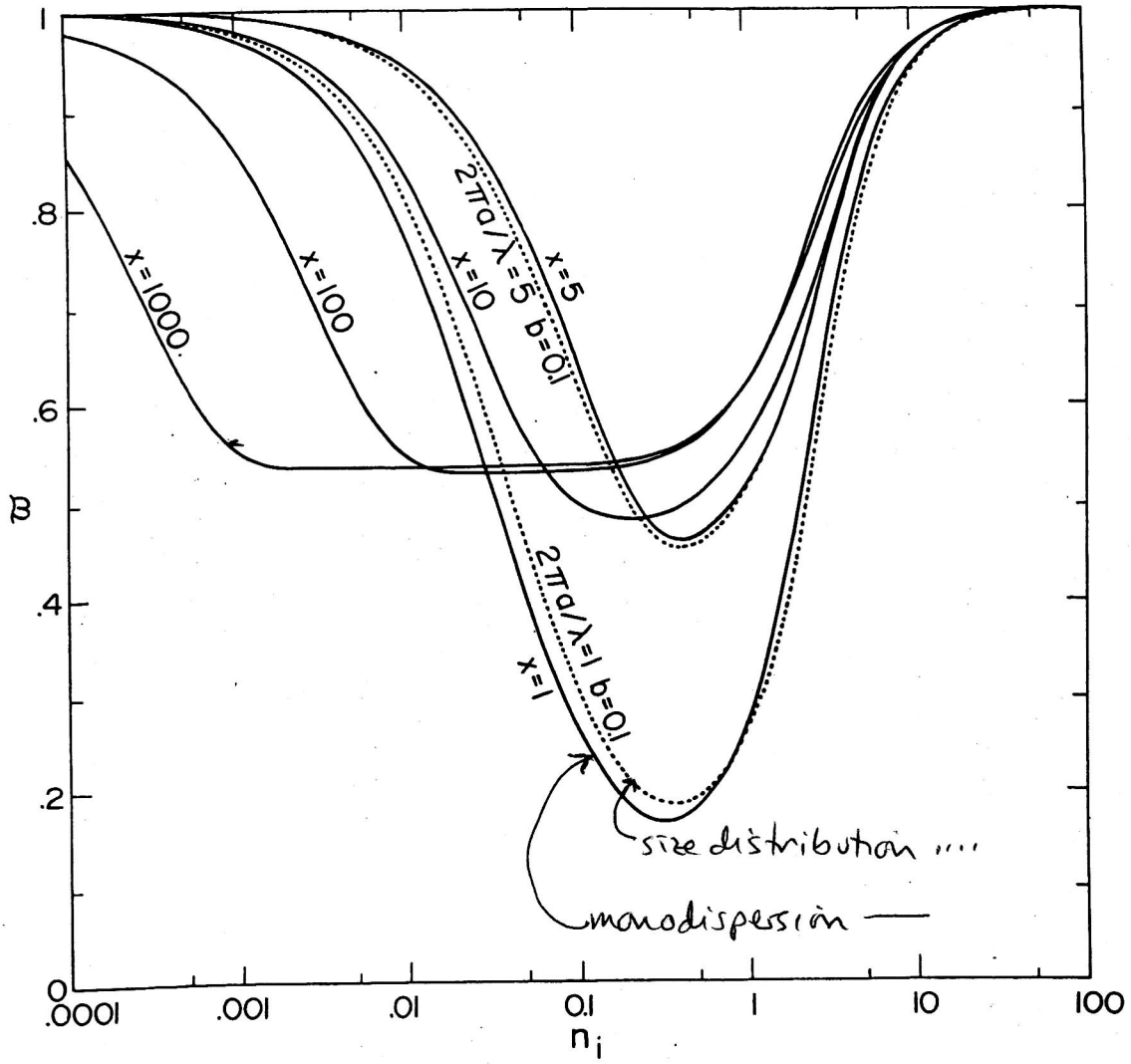

Fig. 10. Single scattering albedo, $\tilde{\omega}$, as a function of the imaginary part of the refractive index, n_i. The solid curves are for $b=0$, corresponding to a single particle so $2\pi a/\lambda = 2\pi r/\lambda \equiv x$. The real refractive index is $n_r = 1.33$.

out as absorption within the particles increases. In geometrical optics the intensity of a light wave traversing a diameter of the sphere is decreased by the factor* e^{-4xn_i}, and thus the major maxima and minima are significantly damped for $4xn_i \sim 1$. The ripples damp out at a value of xn_i which is smaller, but not smaller by orders of magnitude. This is consistent with van de Hulst's (1957) model for the surface wave in which only a few circumvolutions of the sphere are involved.

Figure 9 also shows that as n_i increases Q_{sca} for large particles first decreases, reaches a minimum, and then increases. As n_i becomes large Q_{sca} approaches the value for a perfect reflector, i.e., $Q_{sca} \to 2$ (cf., 2.10).

The dependence of the single scattering albedo $\tilde{\omega}$ on x and n_i is illustrated in Figure 10 for $n_r = 1.33$. The solid curves are each for a single particle of a given size parameter.

* In traveling a distance z the amplitude of the electric field varies as $e^{-ikzn_c} = e^{-ikz(n_r - in_i)}$, and thus the intensity is proportional to e^{-2kzn_i}.

For large x and not too large n_i, $\tilde{\omega}$ approaches ~ 0.53. This can be understood from Figure 4; for $n_i = 0$, 50% of the scattered light is diffracted, 3.3% is reflected and the remainder is refracted into the particle. As long as n_i is small this division of the rays remains approximately correct, and for large particles the refracted light is absorbed within the particle even for small n_i. As x becomes small $\tilde{\omega}$ takes on values less than 0.5, a result of the fact that the Rayleigh region is being approached (cf., 2.19 and 2.20).

The dotted curves in Figure 10 are for a size distribution of significant width, $b = 0.10$ (cf., Figure 7). For $x = 1$ and $x = 5$ there is a non-negligible dependence of $\tilde{\omega}$ on b, as would be expected. However, for $x \geq 10$ $\tilde{\omega}$ is practically independent of the width of the size distribution. Thus for particles this large only one parameter, r_{eff}, is required to define the effect of the particle size distribution on $\tilde{\omega}$. This is a result of our choice of parameters; for example, it can be shown that two different distributions with the same mode radius or the same mean radius in general have considerably different values of $\tilde{\omega}$.

The asymmetry parameter $\langle \cos\alpha \rangle$ is graphed in Figure 11 as a function of $x_{\text{eff}} =$

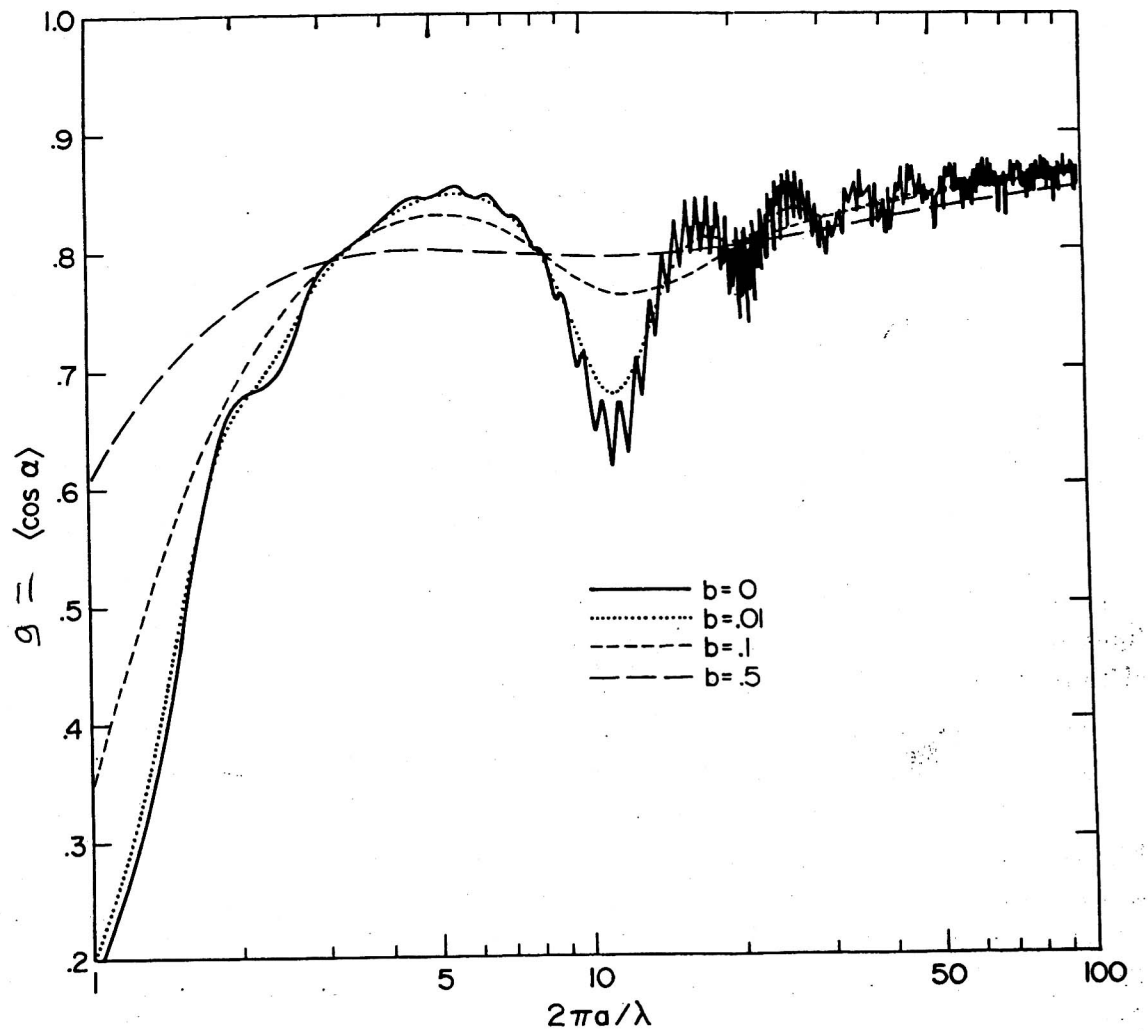

Fig. 11. Asymmetry parameter, $\langle \cos\alpha \rangle$, as a function of the effective size parameter, $2\pi a/\lambda$. The standard size distribution (2.56) was used with four values of the effective variance b. For the case $b = 0$, $2\pi a/\lambda = 2\pi r/\lambda \equiv x$. The refractive index is $n_r = 1.33$, $n_i = 0$.

$2\pi a/\lambda$ for the size distribution (2.56). The refractive index is $n_r = 1.33$. For small particles $\langle \cos\alpha \rangle$ approaches zero, the value obtained for Rayleigh scattering. For large x $\langle \cos\alpha \rangle$ approaches the result which is obtained with the geometrical optics phase function, ~ 0.87 (van de Hulst, 1957). The maxima and minima in $\langle \cos\alpha \rangle$ have the same physical origin as those in Q_{sca} discussed above. $\langle \cos\alpha \rangle$ is thus dependent on x_{eff} and v_{eff}. The dependence of $\langle \cos\alpha \rangle$ on higher moments is small provided $x_{eff} \geqslant 10$. For the range of v_{eff} typical of terrestrial clouds the dependence of $\langle \cos\alpha \rangle$ on v_{eff} is negligible, at least for the range of x_{eff} appropriate for the visible and near-infrared regions.

Figure 12 shows the asymmetry parameter for different real refractive indices. The size distribution is (2.56) with $b = 0.07$, which is sufficient to smooth out all maxima except the primary interference maximum (cf., Figure 8). This maximum in $\langle \cos\alpha \rangle$ corresponds to a maximum in Q_{sca}, since this feature is a result of constructive interference in the forward direction. For the larger values of refractive index $\langle \cos\alpha \rangle$

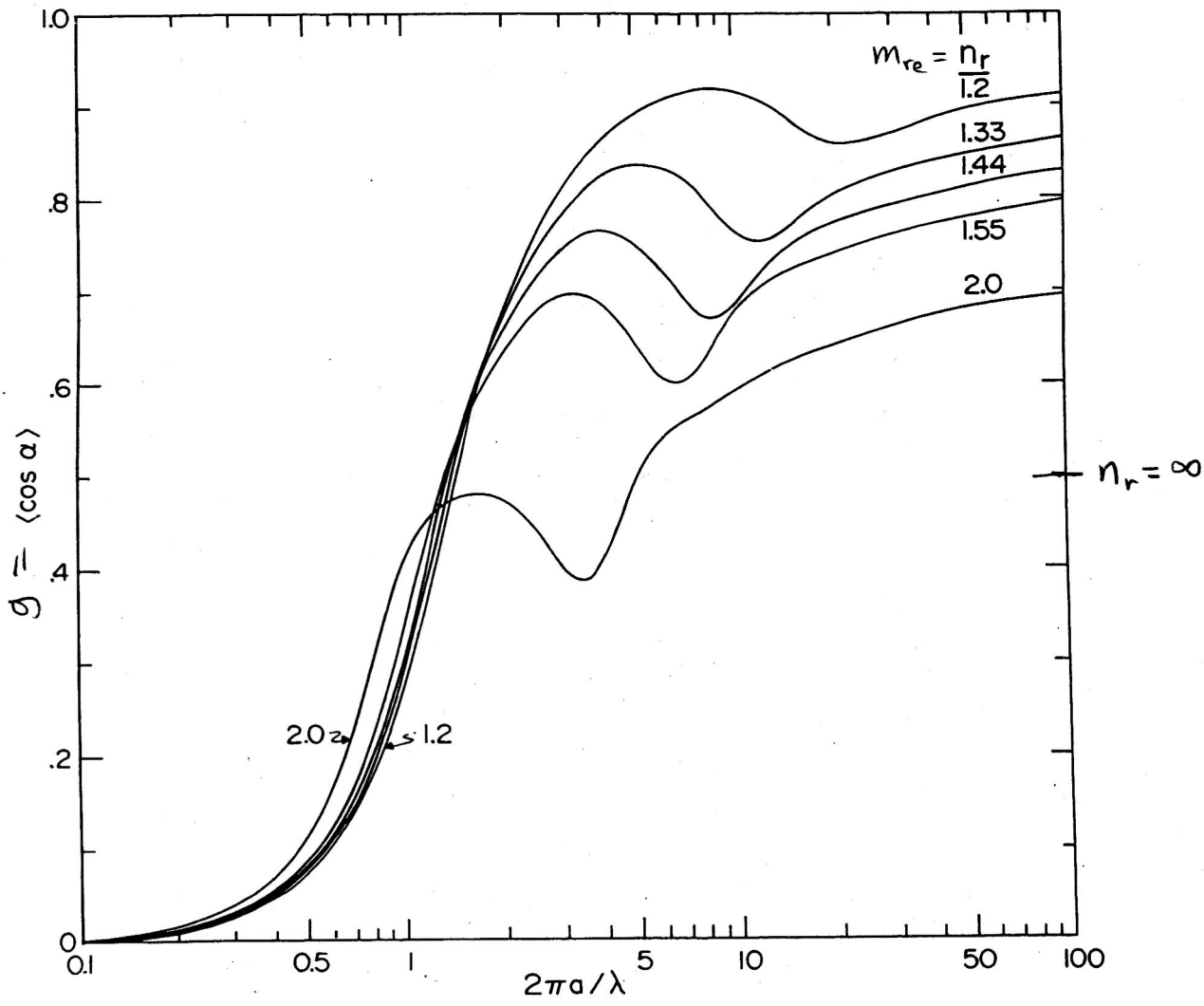

Fig. 12. Asymmetry parameter, $\langle \cos\alpha \rangle$, as a function of effective size parameter, $2\pi a/\lambda$. Results are shown for five values of the real refractive index, n_r, all with $n_i = 0$. The standard size distribution (2.56) was used with $b = 0.07$.

deviates more readily from its zero value for Rayleigh scattering, as expected. At $2\pi a/\lambda = 100$ the limit of $\langle \cos\alpha \rangle$ for geometrical optics has nearly been reached; e.g., for $n_r = 1.33$ the phase function for geometrical optics yields $\langle \cos\alpha \rangle \sim 0.87$. The gradual increase in $\langle \cos\alpha \rangle$ as it approaches its limiting value is due in large part to the decreasing width of the diffraction lobe of the phase function. As $n_r \to 1$, $\langle \cos\alpha \rangle \to 1$ for large $2\pi a/\lambda$, since $n_r = 1$ corresponds to no scattering at all. On the other hand, as $n_r \to \infty$, $\langle \cos\alpha \rangle \to 0.5$ for large $2\pi a/\lambda$, because half of the scattered radiation is diffracted in the forward direction and half is reflected isotropically (cf., 2.10).

Figure 13 illustrates the effect of the imaginary part of the refractive index on $\langle \cos\alpha \rangle$. For $x_{\text{eff}} = 1000$ as n_i increases $\langle \cos\alpha \rangle$ first increases from its geometrical optics value for $n_i = 0$ (~ 0.87); this increase is a result of absorption of rays refracted into the particle. At $n_i = 0.001$ the absorption of refracted rays is essentially complete since in traversing a particle diameter the reduction in intensity is the factor $e^{-4x n_i} = e^{-4}$. Thus only diffraction and reflection contribute and $\langle \cos\alpha \rangle \sim 0.94 \times 1 + 0.06 \times \frac{1}{2} = 0.97$,

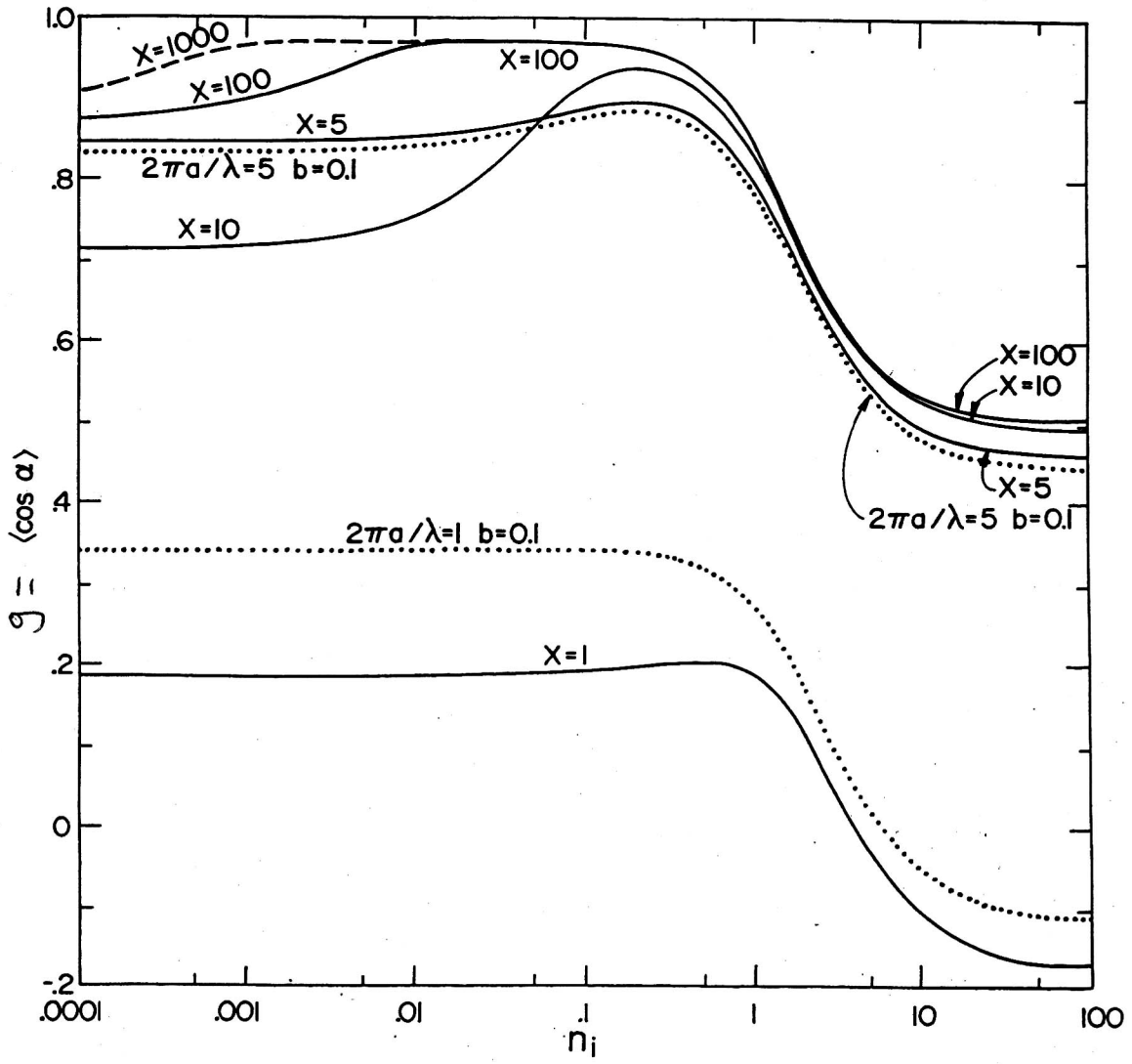

Fig. 13. Asymmetry parameter, $\langle \cos\alpha \rangle$, as a function of the imaginary part of the refractive index, n_i. The solid curves are for $b = 0$, corresponding to a single particle, so $2\pi a/\lambda = x$. The real refractive index is $n_r = 1.33$.

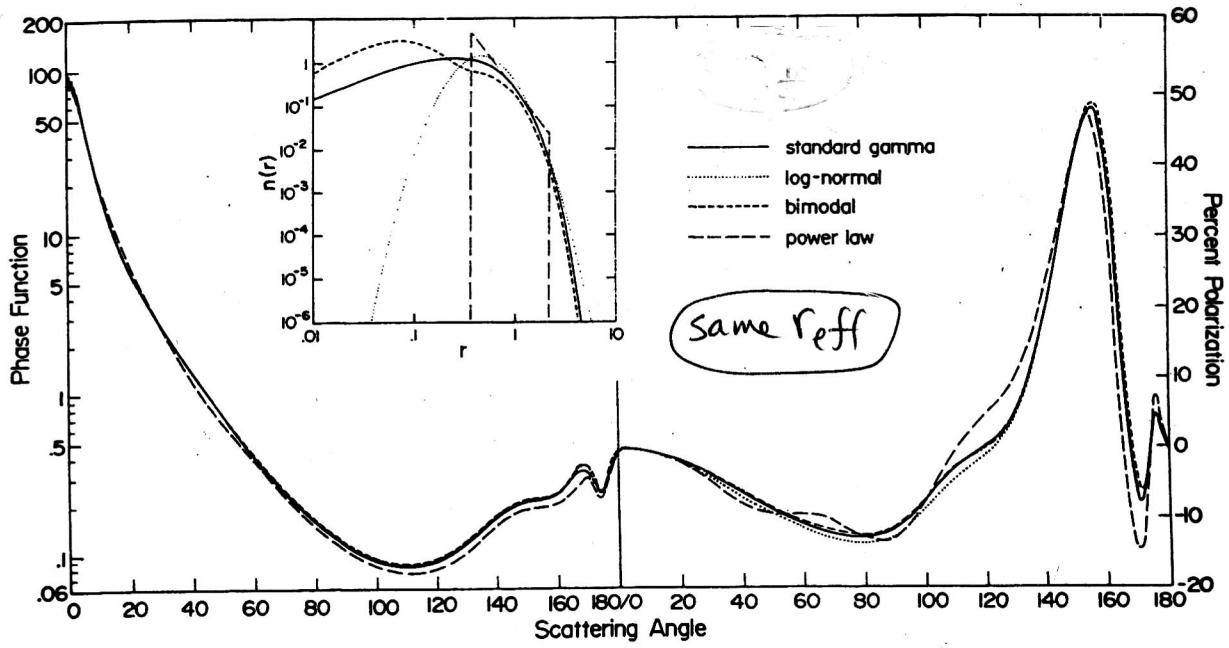

Fig. 14. Phase function, P^{11}, and percent polarization, $-100P^{21}/P^{11}$, for single scattering of unpolarized incident light. Results are shown for the four size distributions illustrated in the inset, all of which have the same value for r_{eff} (1 μ) and v_{eff} (0.25), where r_{eff} is the effective radius and v_{eff} the effective variance. The calculations are for the real refractive index $n_r = 1.33$ and wavelength $\lambda = 0.55$ μ.

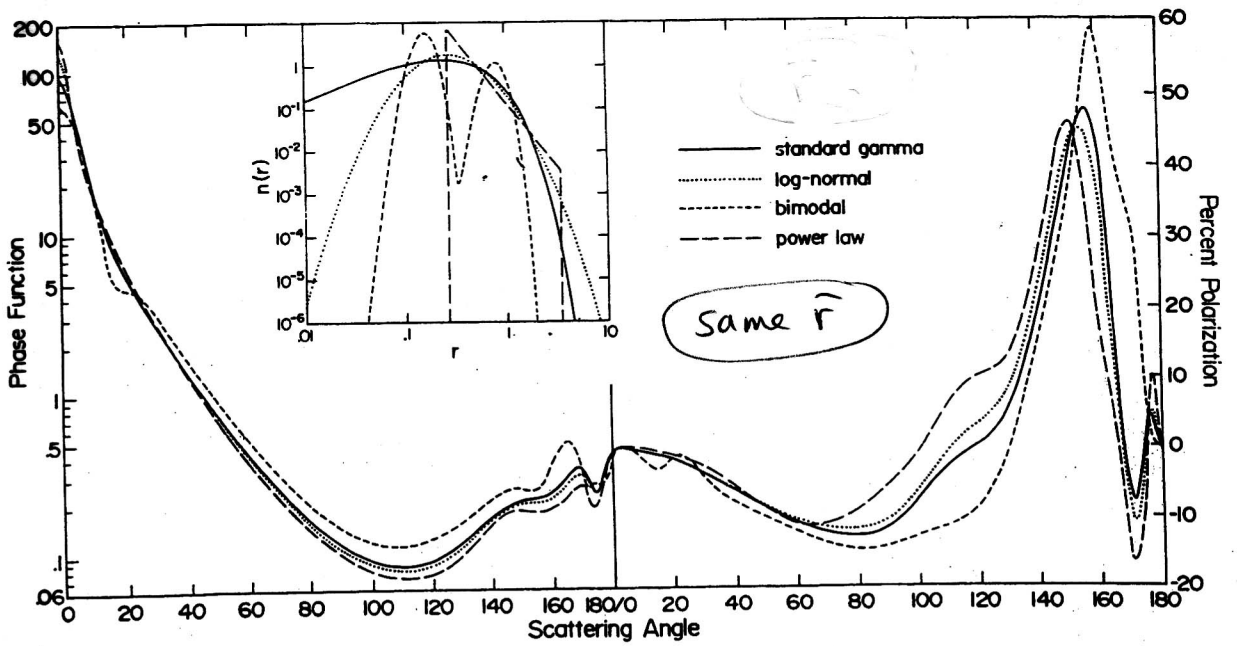

Fig. 15. Phase function, P^{11}, and percent polarization, $-100P^{21}/P^{11}$, for single scattering of unpolarized incident light. Results are shown for the four size distributions illustrated in the inset. The standard gamma distribution is the same as in Figure 14. All four distributions have $\bar{r} = 0.5$ μ and $\sigma^2 = 0.125$ μ^2, where $\bar{r}$ is the mean radius and σ^2 the variance. The calculations are for the real refractive index $n_r = 1.33$ and wavelength $\lambda = 0.55$ μ.

Multiple Scattering of Polarized Light in Planetary Atmospheres. Part II. Sunlight Reflected by Terrestrial Water Clouds

JAMES E. HANSEN

Goddard Institute for Space Studies, NASA, New York, N. Y.

(Manuscript received 3 August 1971, in revised form 23 August 1971)

ABSTRACT

The intensity and polarization of sunlight reflected by terrestrial water clouds are computed with the doubling method. The calculations illustrate that this method can be effectively used in problems involving strongly anisotropic phase matrices. The method can therefore be used to derive information about planetary clouds, including those of the earth, from polarimetric observations.

The results of the computations indicate that the polarization is more sensitive than the intensity to cloud microstructure, such as the particle size and shape. Multiple scattering does not wash out features in the polarization as effectively as it does in the intensity, because the polarization arises primarily from photons scattered once or a small number of times. Hence polarization measurements, particularly in the near infrared, are potentially a valuable tool for cloud identification and for studies of the microphysics of clouds.

The computations are made primarily at four wavelengths in the near infrared, from 1.2 to 3.4 μ. The results for $\lambda = 1.2\ \mu$ are also applicable to scattering at visual and ultraviolet wavelengths. The other wavelengths are selected to illustrate the basic scattering characteristics in the near infrared for reflection of sunlight from water clouds.

It is shown that the intensity computed with the exact theory including polarization differs by $\lesssim 1.0\%$ from the intensity computed in the common scalar approximation in which the polarization is neglected. Therefore, when only the intensity is required, and not the polarization, it is possible in most cases to neglect polarization entirely.

An approximation obtained by setting the phase matrix elements $P^{34}(\alpha)$ and $P^{43}(\alpha)$ equal to zero is proposed and tested. It is found that this introduces errors less than one part in 10^6 for the intensity and errors $\lesssim 0.0002$ in the degree of polarization. This means that in computing the polarization properties for multiple scattering by spherical particles it is usually adequate to work with 3 by 3 matrices.

An examination is made of the accuracy of the polarization in the approximation in which it is assumed that multiply scattered photons are unpolarized. A modified version of this, which, in addition, takes advantage of the fact that diffracted light is nearly unpolarized, is also tested. The modified approximation is found to yield an improved accuracy in most cases.

Another approximation, which can be termed a renormalization method, is described and tested. The method consists of modifying the phase matrix for single scattering so that the integrations over zenith angle can be performed with a small number of points. The order of the approximation (the number of zenith angles in the integrations) can easily be varied and accuracies sufficient for practical applications can be obtained at low orders of approximation. The method is therefore useful for small computers.

1. Introduction

The microphysics of clouds is generally assumed to be intimately connected with the general dynamic and thermodynamic processes in individual cloud bodies, as well as with the synoptics of entire weather systems. An improved understanding of the relations of the microphysics to the meso- and macrophysics is essential to the sciences of both weather prediction and weather modification.

Methods of remotely sensing cloud particle phase and size distribution are needed to help relate the microstructure to the cloud type. Furthermore, with an understanding of these relations in hand, it is possible that measurements from satellites of the microstructure of clouds could be of significant value for weather prediction.

Active methods of remote sensing, for example with radar or lasers, can be used for investigating local cloud systems. However, to obtain information over a wide geographic area with a satellite-borne sensor, it is desirable to use reflected sunlight as the probe. It has already been shown (Blau *et al.*, 1966; Hovis and Tobin, 1967; Hansen and Pollack, 1970) that some information on the cloud microstructure can be obtained by observing the intensity of reflected sunlight in the near infrared. It is likely that the polarization of reflected sunlight is more sensitive than the intensity to cloud microstructure. This paper represents one step

Reprinted from **Applied Optics,** Vol. 19, page 1505, May 1, 1980

(73)
(61)

Improved Mie scattering algorithms

W. J. Wiscombe

Scattering of electromagnetic radiation from a sphere, so-called Mie scattering, requires calculations that can become lengthy and even impossible for those with limited resources. At the same time, such calculations are required for the widest variety of optical applications, extending from the shortest UV to the longest microwave and radar wavelengths. This paper briefly describes new and thoroughly documented Mie scattering algorithms that result in considerable improvements in speed by employing more efficient formulations and vector structure. The algorithms are particularly fast on the Cray-1 and similar vector-processing computers.

I. Introduction

Mie scattering calculations pervade the entire field of atmospheric optics. Applications range from one end of the electromagnetic spectrum to the other—from UV solar radiation backscattered by stratospheric aerosols to satellites, through visible and IR radiation scattered by clouds and aerosols, to microwaves and radar scattered from large hydrometeors.

The actual formulas for Mie scattering are well known.[1,2] The quantities required are

$$Q_{\text{ext}} = \frac{2}{x^2}\sum_{n=1}^{N}(2n+1)\text{Re}(a_n + b_n), \tag{1a}$$

$$Q_{\text{sca}} = \frac{2}{x^2}\sum_{n=1}^{N}(2n+1)(|a_n|^2 + |b_n|^2), \tag{1b}$$

$$g = \frac{4}{x^2 Q_{\text{sca}}}\sum_{n=1}^{N}\left[\frac{n(n+2)}{n+1}\text{Re}(a_n a_{n+1}^* + b_n b_{n+1}^*) + \frac{2n+1}{n(n+1)}\text{Re}(a_n b_n^*)\right], \tag{1c}$$

$$S_1(\mu) = \sum_{n=1}^{N}\frac{2n+1}{n(n+1)}[a_n\pi_n(\mu) + b_n\tau_n(\mu)], \tag{1d}$$

$$S_2(\mu) = \sum_{n=1}^{N}\frac{2n+1}{n(n+1)}[a_n\tau_n(\mu) + b_n\pi_n(\mu)], \tag{1e}$$

which are, respectively, the extinction efficiency, scattering efficiency, asymmetry factor, and complex scattering amplitudes for two orthogonal directions of incident polarization. ($|S_1|^2$ and $|S_2|^2$ are the scattered intensities.) Size parameter x is the sphere's circumference divided by the wavelength. The complex-valued Mie coefficients a_n and b_n depend on x and on the complex refractive index $m = m_{\text{Re}} - im_{\text{Im}}$. They are expressed in terms of spherical Bessel functions; in particular, following Infeld's formulation,[3] they involve the function

$$A_n(mx) = \psi_n'(mx)/\psi_n(mx), \tag{2}$$

where $\psi_n(z) \equiv zj_n(z)$. Finally, μ is the cosine of the scattering angle, and the angular eigenfunctions are

$$\pi_n(\mu) = P_n'(\mu), \tag{3}$$

$$\tau_n(\mu) = \mu\pi_n(\mu) - (1-\mu^2)\pi_n'(\mu), \tag{4}$$

where P_n is a Legendre polynomial.

The only remaining question is how to structure the Mie computation for maximum efficiency, while at the same time maintaining accuracy and avoiding numerical instability and ill-conditioning. The first published Mie algorithms were those of Dave[4,5] although Irvine, Plass, and Cheyney, to name just a few, had been doing Mie calculations for several years prior. Most new investigators in the intervening years tended to use Dave's algorithms or variants thereof.

Mie calculations have gained a reputation for being time-consuming. This is, first, because the upper limit N in Eqs. (1) is roughly equal to x, which can become very large, e.g., about 1260 for a 100-μm water drop at a visible wavelength of 0.5 μm. Second, because in typical applications one wishes to sum these series for a large number of radii (as in integrating over a size distribution) or for a large number of wavelengths (as in integrating across the solar spectrum) or for a large number of refractive indices (as in inverting scattering measurements to deduce refractive index). The present author alone has used many hours of Univac 1108, IBM 360/91, CDC 7600, and Cray-1 time doing Mie computations.

The author is with National Center for Atmospheric Research, Boulder, Colorado 80307.
Received 12 December 1979.
0003-6935/80/091505-05$00.50/0.

(74)

NCAR/TN-140+STR
NCAR TECHNICAL NOTE

June 1979

Mie Scattering Calculations: Advances in Technique and Fast, Vector-Speed Computer Codes

Warren J. Wiscombe

ATMOSPHERIC ANALYSIS AND PREDICTION DIVISION

NATIONAL CENTER FOR ATMOSPHERIC RESEARCH
BOULDER, COLORADO

(75)

Efficiency Factors in Mie Scattering

H. M. Nussenzveig[a]
Cooperative Institute for Research in the Environmental Sciences, Boulder, Colorado 80309, and National Center for Atmospheric Research, Boulder, Colorado 80307

and

W. J. Wiscombe
National Center for Atmospheric Research, Boulder, Colorado 80307

(Received 22 May 1980)

Asymptotic approximations to the Mie efficiency factors for extinction, absorption, and radiation pressure, derived from complex-angular-momentum theory and averaged over $\Delta\beta \sim \pi$ (β = size parameter), are given and compared with the exact results. For complex refractive indices $N = n + i\kappa$ with $1.1 \leq n \leq 2.5$ and $0 \leq \kappa \leq 1$, the relative errors decrease from ~(1–10)% to ~(10^{-2}–10^{-3})% between $\beta = 10$ and $\beta = 1000$, and computing time is reduced by a factor of order β, so that the Mie formulae can advantageously be replaced by the asymptotic ones in most applications.

PACS numbers: 42.20.Gg, 42.68.Vs

The Mie efficiency factors[1] for extinction (Q_{ext}), absorption (Q_{abs}), and radiation pressure (Q_{pr}) are just the corresponding cross sections divided by the projected area πa^2 of the scattering sphere. These quantities are important in many applications. Typical size parameters $\beta = ka$ (k = wave number, a = droplet radius) range from $\ll 1$ up to ~10^4, with complex refractive indices $N = n + i\kappa$, $1.1 \lesssim n \lesssim 1.9$, $10^{-9} \lesssim \kappa \lesssim 1$. The efficiencies vary extremely rapidly[2] with β, n and κ; but in most applications one is only interested in means $\langle Q \rangle$ over some range $\Delta\beta$, not in this high-frequency "ripple."

Evaluation of the exact Mie expressions[1] requires summing ~β partial waves. Upon integration across size or wavelength with a step fine enough to resolve the ripple ($\Delta\beta \leq 0.01$–0.1), one is faced with exorbitant computation times. Approximations[1] based on geometrical optics and classical diffraction theory do not have the required accuracy until β exceeds several thousand (cf. below). Clearly, better approximations, devoid of ripple, are needed.

The complex-angular-momentum theory of Mie scattering[3] can furnish such approximations. By a simple extension of previously developed tech-

S. Warren

(76)

Algorithms for the calculation of scattering by stratified spheres

Owen B. Toon and T. P. Ackerman

Efficient, numerically stable, methods for the calculation of light-scattering intensity functions for concentrically coated spheres are discussed. Earlier forms of these equations are subject to various numerical difficulties which give rise to significant errors, especially for thin absorbing shells. The present equations are accurate for all refractive indices, for large and small particles, and for cores with any relative size.

I. Introduction

Theoretical expressions describing the light scattered by a particle composed of a spherical core surrounded by a concentric shell were developed many years ago by Aden and Kerker[1] and have been discussed in detail by Kerker.[2] Investigators have encountered several numerical problems using these equations, which we attempt to overcome in this paper.

Espenscheid *et al.*[3] found that the use of upward recursion to evaluate the Bessel functions which appear in Kerker's equations produced large errors. Kattawar and Hood[4] found that the higher-order terms in the expansions for the scattered radiation field were subject to error because one must subtract large nearly equal terms which can result in a numerically meaningless remainder. Ackerman and Toon,[5] who studied scattering by particles slightly larger than the wavelength of light, which were covered by thin carbon shells, found that even the first term in the expansion for the scattered radiation field could be numerically invalid because of the subtraction of large quantities to obtain a smaller one. In addition to these problems, Kerker's equations contain spherical Bessel functions whose magnitude increases exponentially with their argument and may easily exceed the capacity of modern computers. To circumvent these various difficulties, we have reformulated Kerker's[2] equations using many of the same techniques employed to prevent similar problems which arise in the equations for scattering by homogeneous spheres.[2]

We shall first describe the equations we use to calculate the scattered radiation field and discuss their numerical stability. Then we present the schemes we use to find the various terms which appear in the equations and illustrate the numerical stability of these schemes. Finally, we describe the checks we have performed to be certain that our complete computer code is numerically stable and accurate.

II. Computational Equations

The scattered radiation field is completely determined by a series of coefficients which Kerker[2] denotes by a_n and b_n. For example, the extinction coefficient is given by

$$Q_{ext} = \left(\frac{2}{\alpha^2}\right) \sum_{n=1}^{\infty} (2n + 1)[\mathrm{Re}(a_n + b_n)], \quad (1)$$

where α, the size parameter, is the product of π and the ratio of the particle diameter to the wavelength of light. The symbol Re denotes the real part of the complex quantity $a_n + b_n$.

Kerker's equations for a_n and b_n contain three Ricatti-Bessel functions and their derivatives. To obtain a numerically stable form of Kerker's equations, we performed four operations. First, we divided all the equations by the appropriate terms to replace the Ricatti-Bessel functions with their logarithmic derivatives. This technique, long used in standard Mie theory, circumvents the exponential dependence of the functions on size parameter. Second, we formed ratios of the terms in the equations which could not be expressed as logarithmic derivatives, so that the ratios are bounded as the size parameter becomes large and as the core size becomes small. Third, we eliminated many of the Ricatti-Bessel functions by using the fundamental relations between them. Most of the problems in the original equations due to the subtraction of large terms to leave a small residual were caused by two Ricatti-Bessel functions converging to similar values. Analytically expressing the Bessel functions in terms of each other eliminates these problems. Finally, to calculate

The authors are with NASA Ames Research Center, Space Science Division, Moffett Field, California 94035.

Received 11 April 1981.

Reprinted from JOURNAL OF THE ATMOSPHERIC SCIENCES, Vol. 43, No. 5, 1 March 1986
American Meteorological Society

To Steve with best regards. Thanks for your help on this one.
Craig

Applicability of Effective-Medium Theories to Problems of Scattering and Absorption by Nonhomogeneous Atmospheric Particles

CRAIG F. BOHREN

Dept. of Meteorology, Pennsylvania State University, University Park, PA 16802

(Manuscript received 9 April 1985, in final form 24 September 1985)

ABSTRACT

Effective-medium theories yield effective dielectric functions (or, equivalently, refractive indices) of composite media. Such theories have been formulated that go beyond the Maxwell-Garnett and Bruggeman theories, which are restricted to media composed of grains much smaller than the wavelength. These extended effective-medium theories do not, however, yield effective dielectric functions that can be used for the same purposes for which we unhesitatingly use the dielectric functions of substances such as pure water and pure ice (e.g., reflection and transmission by smooth interfaces; absorption and scattering by particles). Extended dielectric functions can lead to unphysical results; for example, absorption in composite media with nonabsorbing components. Moreover, if the grains in composite media are large enough to give rise to magnetic dipole and higher-order multipole radiation, then the effective permeability of the composite medium cannot be taken to be that of free space even if the grains are nonmagnetic.

Recently, extended effective-medium theories have been applied to the problem of determining the effective dielectric function of ice in which soot grains are embedded in order to explain a factor of 2 discrepancy between measurements of the albedo of soot-contaminated snow and calculations based on a snow albedo model. Setting aside questions about the applicability of these theories, reasonable alternative explanations for the discrepancy exist: (i) Soot is not an invariable substance; measured refractive indices of carbonaceous materials vary appreciably, especially the imaginary part (about a factor of 5). (ii) Absorption by a small soot particle depends on its shape, varying by as much as a factor of 2. (iii) Absorption by a soot particle may be enhanced by porosity; for a fixed particle volume, the enhancement is roughly proportional to the porosity. To predict exactly how much a given amount of soot reduces the visible albedo of snow requires, therefore, more detailed information about the soot than is likely to be readily obtainable.

1. Introduction

Some particles in the atmosphere are nonhomogeneous, which leads to questions about how one calculates absorption and scattering by them. One example is determining radar backscattering cross sections of melting snowflakes and spongy-ice hailstones (Bohren and Battan, 1980, 1982; Battan and Bohren, 1982, Chýlek et al., 1984a). In recent papers by Chýlek et al. (1983, 1984b) the particles considered are inhomogeneous by virtue of embedded soot grains. Since interest in nonhomogeneous atmospheric particles seems to be on the rise, the time has come for a critical look at effective-medium theories. This is particularly important because, as will be shown, serious errors can occur when effective-medium concepts are used uncritically outside their limited domain of validity.

An example of an effective-medium theory is one that gives the dependence of the effective dielectric function of a two-component mixture on the dielectric functions of the components and their volume fractions. Such theories have a long history (Landauer, 1978) predating the publication of Maxwell's *A Treatise on Electricity and Magnetism*. Subsequently, effective-medium theories (or mixing rules) have been turned out steadily, some with solid theoretical foundations, others based on no more than empirical fits to limited sets of data. There is now a bewildering array of them in the scientific literature, although sometimes the differences among them are more apparent than real (e.g., see Bohren and Battan, 1980). Two of these, the Maxwell-Garnett (1904) and the Bruggeman (1935) theories, have had the widest use.

According to both the Maxwell-Garnett and the Bruggeman theories, the effective, or average, dielectric function ϵ_{av} of a two-component mixture depends on only the dielectric functions of its components and their volume fractions:

$$\epsilon_{av} = F(\epsilon, \epsilon_m, f),$$

where f and $1 - f$ are the volume fractions of the components with dielectric functions ϵ and ϵ_m. In the Bruggeman theory F is symmetric with respect to interchange of the components, whereas in the Maxwell-Garnett theory it is not:

$$F(\epsilon, \epsilon_m, f) = F(\epsilon_m, \epsilon, 1 - f), \quad \text{Bruggeman}$$

$$F(\epsilon, \epsilon_m, f) \neq F(\epsilon_m, \epsilon, 1 - f), \quad \text{Maxwell-Garnett.}$$

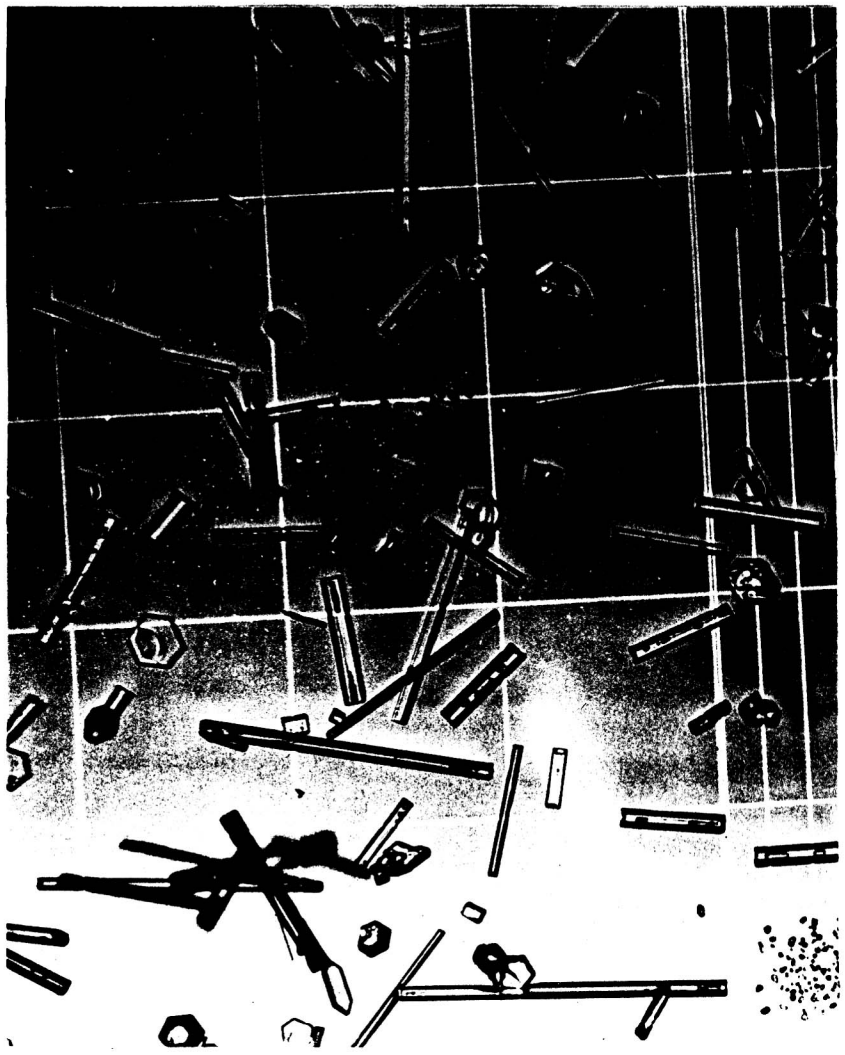

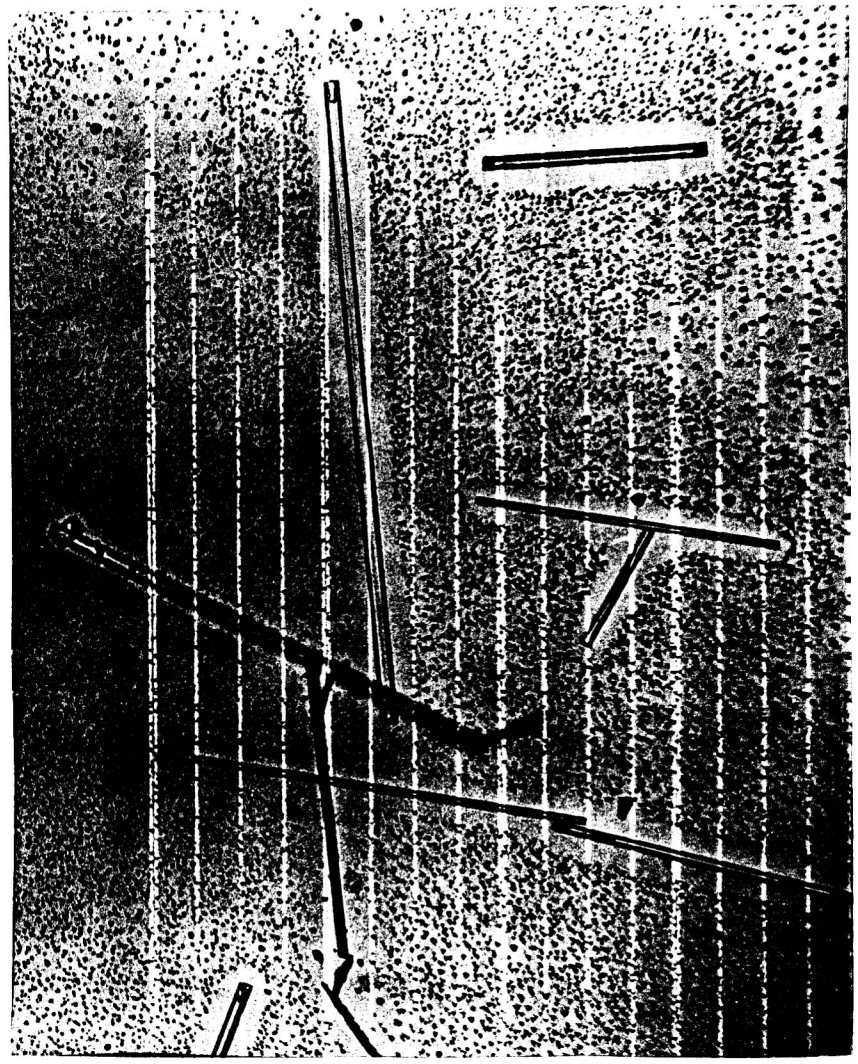

Figure 1

Grenfell & Warren 1999, submitted to J. Geophys. Res. 104 31697-31709

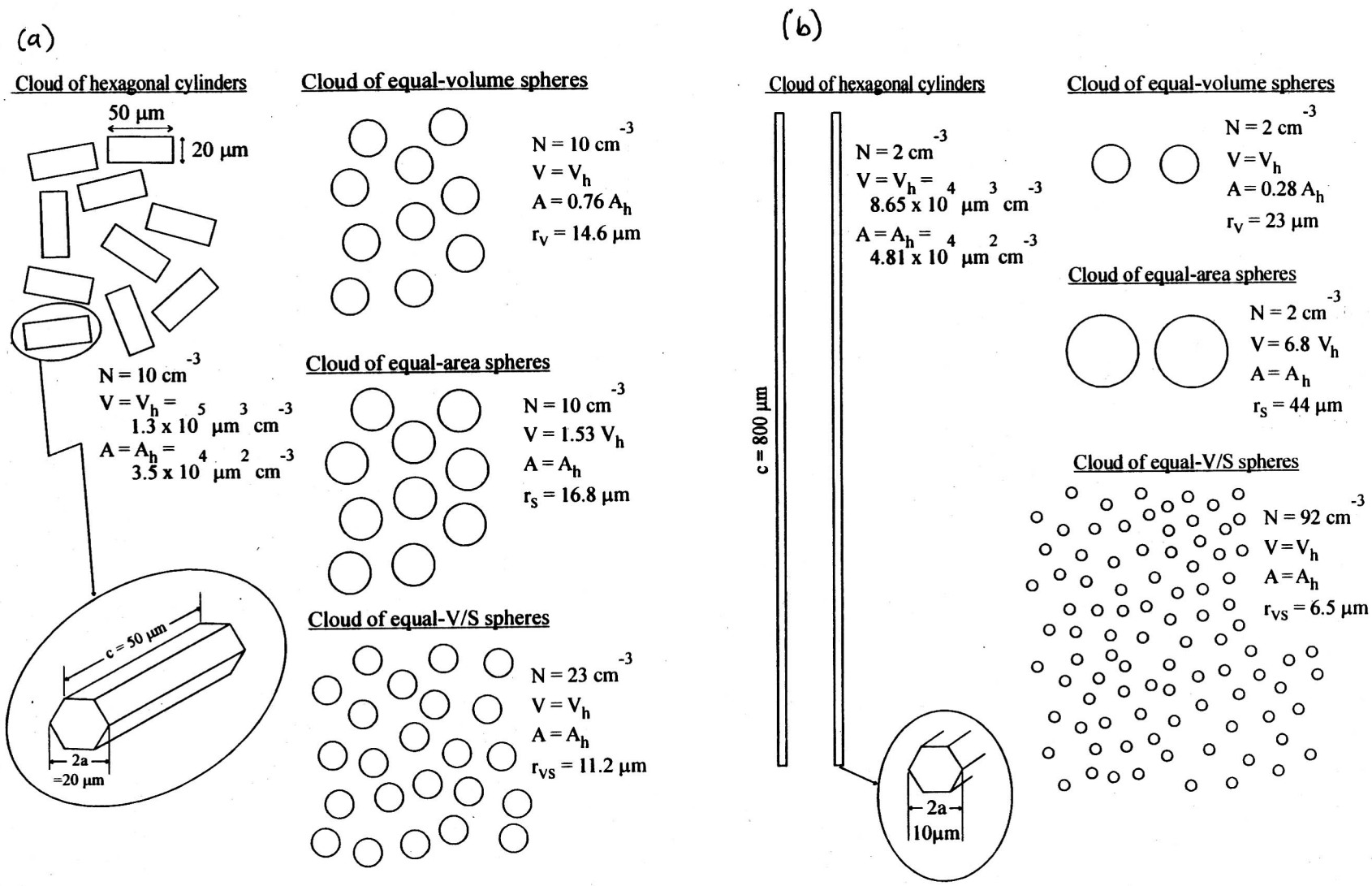

Figure 2


1 mm